THE PENNSYLVANIA STATE UNIVERSITY

IONOSPHERIC RESEARCH

Scientific Report No. 240

SOLAR IONIZING FLUX AS DETERMINED FROM SUNRISE MEASUREMENTS OF ELECTRON CONTENT

by

A. A. Gran

May 30, 1965

GPO PRICE $ _____

OTS PRICE(S) $ _____

Hard copy (HC) 2.00

Microfiche (MF) .75

N65 28541

ACCESSION NUMBER

FACILITY FORM 602

IONOSPHERE RESEARCH LABORATORY

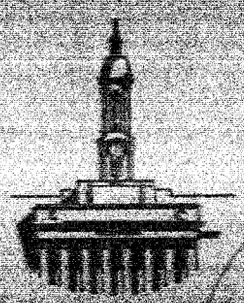

University Park, Pennsylvania

NASA Grant NsG-114-61

Ionospheric Research

NASA Grant NsG-114-61

Scientific Report

on

"Solar Ionizing Flux as Determined from Sunrise Measurements of Electron Content"

by

A. A. Gran

May 30, 1965

Scientific Report No. 240

Ionosphere Research Laboratory

Submitted by: W. J. Ross by J. J. Gibbons
W. J. Ross, Professor of Electrical Engineering

Approved by: A. H. Waynick by J. J. Gibbons
A. H. Waynick, Professor of Electrical Engineering
Director, Ionosphere Research Laboratory

The Pennsylvania State University

College of Engineering

Department of Electrical Engineering

Table of Contents

Page

Abstract

28541

A means of determining solar ionizing flux from sunrise measurements of the increase of electron content at an equatorial station is discussed. The technique is applied to Transit 4-A Faraday Rotation observations made in Peru from September 1961 to February 1963.

It is found that errors well in excess of 20% in electron production rates result from neglect of atomic oxygen ion losses. With this correction, the effective ionizing fluxes were with one exception, about 2×10^{14} ph m^{-2} sec^{-1}. These effective ionizing fluxes represent one half to one third of the total fluxes obtained by photometric methods in the 1027-10A range.

Results of a model study of production are used to convert the effective ionizing fluxes into total fluxes. Comparison of these total fluxes with those obtained by photometric measurements suggest that on the average three photons are required to produce two free electrons, and that N_2^+ and possibly O_2^+ are in general lost by rapid recombination during the sunrise period. Author

Chapter I

Introduction

1.1 The Ionosphere

Since 1902 when Kennelly and Heaviside first postulated the existence of an ionized layer in the upper atmosphere, which might be produced by ionization of the atmospheric gases by ultraviolet radiation from the sun, an intensive study of it has been undertaken. While much has been learned about its characteristics, the depth of study has revealed the complexity of the medium with even many of its principal features yet not fully understood.

It is known that the ionization varies with altitude, latitude, longitude, time of day, season, sunspot cycle and is subject to a variety of irregular and random disturbances.

The region of the atmosphere with which we are primarily concerned in this study, ranges in altitude from 100 to 400 km. Near the ground the atmospheric constituents are principally molecular nitrogen, molecular oxygen and to a much lesser extent, carbon-dioxide. The first two also constitute a major portion of the neutral constituents present above 100 km and are joined with atomic oxygen, which becomes significant due to dissociation of molecular oxygen by solar radiation.

A considerable portion of the knowledge of this region comes through a study of the density distribution of free electrons. The primary source of these electrons is the photoionization of molecular oxygen, atomic oxygen and molecular nitrogen through the reactions

$$O_2 + h\nu \rightarrow O_2^+ + e \qquad \lambda < 1027A$$

$$O + h\nu \rightarrow O^+ + e \qquad \lambda < 910A$$

$$N_2 + h\nu \rightarrow N_2^+ + e \qquad \lambda < 796A$$

$$N_2 + h\nu \rightarrow N + N^+ + e \qquad \lambda < 510A$$

Consequently, the ionization is produced by X-ray and ultraviolet radiation of wavelengths less than 1027 anstroms. The distribution and variation of the solar flux for this wavelength region is extremely complicated, thus making a detailed study of ionospheric reactions difficult.

Numerous mechanisms also exist whereby free electrons are lost, some of which will be dealt with later. Work has been done on the ionospheric processes by many investigators; however, the various works listed in the bibliography by Nicolet and Swider provide an excellent insight to the problem.

1.2 Electron Density Measurements

Several techniques have been developed for determining electron distribution, two of which are of particular interest in this work and consequently will be described briefly.

The method employed longest is that of radio sounding. This consists of sending a pulsed radio wave from the ground to the ionosphere. A pulse of radio waves entering a region of free electrons is reflected when the density of the electrons reaches a critical value proportional to the square of the radio frequency. By measuring the delay time for an echo to return one obtains a measure of the height of the reflecting region. Thus, by noting the delay time and

frequency it becomes possible to obtain electron density height profiles for heights up to the maximum density (F region maximum). More recently the ionosphere has been sounded from above by use of satellites to obtain profiles for the region above the F maximum.

Another method is that known as Faraday rotation. Our concern with it will be in connection with satellite radio beacon sources. This technique is based on the fact that the plane of polarization of a radio wave in traversing the ionosphere is rotated. This is due to a phase path difference between the two opposite circularly polarized modes, which travel with different phase velocities and thus produce a rotation in the resultant plane of polarization. If it is assumed that the ionosphere does not vary horizontally and that the ray is straight, the total angle of rotation is given as

$$\Omega = \frac{K}{f^2} \int B_L N \sec \chi' \, dh \quad ,$$

where

N = electron density at height h

$K = \dfrac{e^3}{8\pi^2 m^2 c \varepsilon_o} = 2.36 \times 10^4$ (rat. mks.)

f = wave frequency

χ' = zenith angle of ray path

dh = element of height

B_L = component of the magnetic field along the ray path

It has been indicated by Browne, Evans, Hargreaves, and Murray

(1956) that $B_L \sec \chi'$ may be considered constant along a given ray path for a wide range of conditions. Thus the expression commonly used for Faraday rotation is

$$\Omega = \frac{K}{f^2} \overline{B_L \sec \chi'} \int N\,dh \quad ,$$

where $\overline{B_L \sec \chi'}$ is an appropriate mean value and $\int N\,dh$ is the number of electrons in a one meter square column extending through the ionosphere to the height of the satellite source. Thus, the total angle of rotation is a measure of the integrated electron density.

1.3 Solar Radiation Measurements

To interpret the electron distributions observed it is imperative that we possess knowledge of the intensity, distribution, and variation of the solar radiation. Efforts to study the ultraviolet radiation from the sun have been severely limited by the power of the earth's atmosphere to absorb all ultraviolet radiation below 1950A before it reaches the ground. The solution has been to make observations within the absorbing region itself. This is most commonly done by flying instruments in rockets. The first direct observations were accomplished in 1946 with the aid of a spectrograph carried aloft in a V-2 rocket. However, most work of this nature has been done since the late fifties. Three principal methods have been developed. The first two utilize spectrographs in which the measurement of the radiation is accomplished by photographic registration or by photoelectric scanning, each of which has its distinct advantages and disadvantages. Non-dispersive measurements

are made by photometers sensitive to narrow spectral intervals, and constitute the third method. The interested reader is referred to a recent summary on this subject by Tousey (1963).

Though the solar emission spectrum is identified in almost complete detail to the shortest wavelength, our knowledge of the intensities is still subject to large uncertainties. Individual rocket measurements have been relatively infrequent. The temporal differences observed are certainly partly real, but also the result of imprecise calibration techniques. Much progress has been made and with the advent of satellites, platforms for more continuous solar monitoring in greater spectral detail have been built.

1.4 Proposed Radiation Measurement

While each of the foregoing methods is meritorious, they all possess shortcomings, and hence another approach to the problem seems worthy of consideration.

Since the ionization is produced by solar radiation, one might expect to be able to determine the intensity of the radiation producing the ionization providing one is able to measure the rate at which ionization takes place, or equivalently, the rate at which electrons are produced. The proposed solution is to measure the rate of change in integrated electron density by means of the Faraday rotation technique, and to account for the rate at which electrons are lost. The production rate is then given by the continuity equation

$$q = \frac{dN}{dt} + L \quad ,$$

where

q = production rate

$\frac{dN}{dt}$ = rate of change of electron density

L = loss rate

The problem of loss is minimized by selecting conditions under which loss is minimal; namely, during sunrise at low magnetic latitudes, and thus the rate of change of electron density is mostly due to production.

The relationship between the solar ionizing flux and the rate of electron production in a vertical column extending through the ionosphere is developed. For purposes of comparison a model study of photon flux and production is also presented. The method is applied to experimental data taken at Huancayo, Peru from the Transit 4-A satellite.

1.5 Previous Sunrise Study

A somewhat similar approach was made by Rishbeth and Setty (1961) who investigated the behavior of the ionospheric F layer at sunrise based on records made in England in 1953-1958. Rough estimates of the flux of ionizing photons were made by deriving the production rates from observed changes in electron density as determined by a series of bottomside soundings of the ionosphere made at short intervals of time.

Chapter II

Development of Working Equations

2.1 Production and Ionizing Flux Relationship

The relationship between production and ionizing flux may be seen if we treat the atmospheric density distribution as exponential (a good approximation) and the incident flux as monochromatic. One then arrives at the well known Chapman production function (Chapman 1931a) for a plane stratified atmosphere.

$$q = \gamma A \rho_o I_\infty \exp \left[\left(-\frac{h}{H} - A\rho_o H (\sec \chi) \exp \left(-\frac{h}{H}\right)\right)\right] ,$$

where

q is the production rate per unit volume at a given height h.

γ is the ionization efficiency factor

A is the mass absorption coefficient

I_∞ is the intensity of the incident radiation

ρ_o is the mass density at the height (h = 0)

χ is the solar zenith angle

H is the scale height (kT/mg)

If one integrates the production rate over all heights from ground to infinity one finds the total production rate in a vertical column. We define this as

$$\int_{\text{ground}}^{\infty} q \, dh \equiv q_T = \frac{\gamma I_\infty}{\sec \chi}$$

This function is good for small zenith angles, but under sunrise conditions the secant factor no longer holds, since the atmosphere can no longer be treated as plane stratified.

A production function for a spherically stratified atmosphere useful under sunrise conditions was derived by Chapman (1931b). Similar vertical integration of this function is much more complex, since the analog of sec χ is what is called the Chapman function

$$Ch(H, \chi) = X \sin \chi \int_0^{\chi} \exp \left\{ X (1 - \sin \chi / \sin \lambda) \right\} \csc^2 \lambda \, d\lambda \quad ,$$

where $X = p/H$ and p is the distance from the center of the earth to the point where production is sought.

Since vertical integration of the production function in closed form is virtually impossible we refer to values of the Chapman function computed by Wilkes (1954). We note that for a constant scale height the value of X at a height of 0 and 600 km differs less than 5% from that at 300 km. This small change in X produces only about a 2% change in the Chapman function over that height range. Consequently, for a given solar zenith angle we are justified in treating the Chapman function as constant with height. When this is done we get upon integrating vertically a result similar to before, namely,

$$q_T = \frac{\gamma I_\infty}{Ch(H, \chi)} \quad .$$

Discussion thus far has only been concerned with a single constituent atmosphere and monochromatic radiation. For the real situation of a multiconstituent atmosphere and chromatic radiation

the production rate at a given height is given by

$$q_h = \sum_{\lambda} \left(\sum_j \sigma_j' \, n_j \right)_\lambda I_{\infty\lambda} \exp \left(- \sum_{\lambda} \sigma_j N_j \right)_\lambda \quad ,$$

where

λ denotes wavelength

j denotes constituent

n - particle density at given height

N - number of particles in a square absorbing column above h, (along the ray path "S")

σ - total absorption cross section

σ' - photoionization cross section

$I_{\infty\lambda}$ - the number of incident photons of wavelength λ at the top of the atmosphere

Generally, $n_j = n_{oj} \exp(-h/H_j)$, so we may write

$$N_j = \int n_j \, dS \simeq \int n_{oj} \exp(-h/H_j) \left\{ \begin{matrix} \sec \chi \\ Ch(H, \chi) \end{matrix} \right\} dh$$

Also, of later importance, the ratio $\sigma'/\sigma = \gamma$ is the ionization efficiency of the radiation.

2.2 Production and Simple Theory Approximation

Clearly, such a complete description of the production process is extremely complex and not fully understood, especially in terms of appropriate values for the various quantities. Consequently, we shall endeavor to apply the simple theory using an expression of the form presented earlier, in which the flux is an effective ionizing

radiation producing an electron distribution similar to what is observed. This requires, of course, that we attribute an effective scale height to the atmosphere. Under these conditions the Chapman function will give the relationship for variation of production with zenith angle, and the expression previously derived for the production rate in a vertical column can then be used.

Chapter III

Considerations of Loss

3.1 Electron Diffusion

Electron production is accompanied by several loss mechanisms which contribute to the rate of change of electron content. Diffusion of electrons from one region to another constitutes one loss process. Rishbeth (1961) considered diffusion of ionization in the sunrise F-layer and found little indication for vertical drift velocities, due to electromagnetic forces, influencing the rates of increase of electron density observed at sunrise. Since a vertical integration is being made vertical diffusion will be of no significance. Furthermore, in the absence of sufficient information and to avoid undue complexity horizontal diffusion will be considered to be negligible in this work.

3.2 Electron Recombination

There are two principal ways in which electrons may be lost by combination with positive ions in the ionosphere. Radiative recombination occurs according to

$$X^{+} + e \rightarrow X' + h\nu \quad ,$$

where the electron combines with an atomic ion. In dissociative recombination the electron combines with molecular ions by the process

$$XY^{+} + e \rightarrow X' + Y' \quad ,$$

where the primes indicate the various possible excited states.

Radiative recombination processes are ignored since they are a much slower process than dissociative recombination (Swider 1963).

The rate at which dissociative recombination occurs is commonly given as αn^2, where α is the effective recombination coefficient and n is the electron density. Various experimental determinations of $\alpha(N_2^+)$, $\alpha(O_2^+)$ and $\alpha(NO^+)$ exist; however, the values differ widely as can be seen in Nicolet and Swider (1963) and in Friedman (1964) where some of the values are discussed and tabulated.

Atomic oxygen is the major ionized constituent and it is generally accepted that the loss process in the F region is one of charge exchange with molecular nitrogen and molecular oxygen followed by dissociative recombination according to

$$O^+ + \begin{bmatrix} O_2 \\ N_2 \end{bmatrix} \rightarrow \begin{bmatrix} O_2^+ \\ NO^+ \end{bmatrix} + \begin{bmatrix} O \\ N \end{bmatrix}$$

$$\begin{bmatrix} O_2^+ \\ NO^+ \end{bmatrix} + e \rightarrow O + \begin{bmatrix} O \\ N \end{bmatrix}$$

It was shown by Ratcliffe (1956) that this dual loss mechanism results in the loss term

$$L = \frac{\alpha \beta n^2}{\alpha n + \beta} ,$$

where

α = quadratic loss coefficient, $cm^3\ sec^{-1}$

β = linear loss coefficient, sec^{-1}

n = electron density, cm^{-3}

3.3 Loss Minimization

In view of the difficulty of determining loss rates accurately, it is highly desirable to minimize this contribution to the rate of change of electron density. It is known that at low magnetic latitudes ionization is reduced almost completely by sunrise, especially at lower altitudes, to approximately 1/20 of daytime values. Due to this low ionization, electron loss rates are minimal and consequently, the change in electron density is primarily due to production. Under such conditions the rate of change of electron density is very large as can be seen from the vertical sounding electron density profiles, Figure 1, made at Huancayo, Peru during sunrise at 15 minute intervals. It is seen that in the thirty minute interval the electron density nearly doubles in the lower ionosphere.

3.4 E-Region Losses

We might note that as was indicated by Setty, Smith and Bourne (1964) that the value of $3 \times 10^{-8}\ cm^3\ sec^{-1}$ has been adopted by several workers as the rate coefficient for the dissociative recombination of O_2^+, which is believed to be the primary loss process in the E region. However, to use this value it is necessary to assume an electron production rate at night to account for the observed nearly constant value of total ionization below the F region for at least 3 to 4 hours before sunrise. Otherwise the coefficient must be much

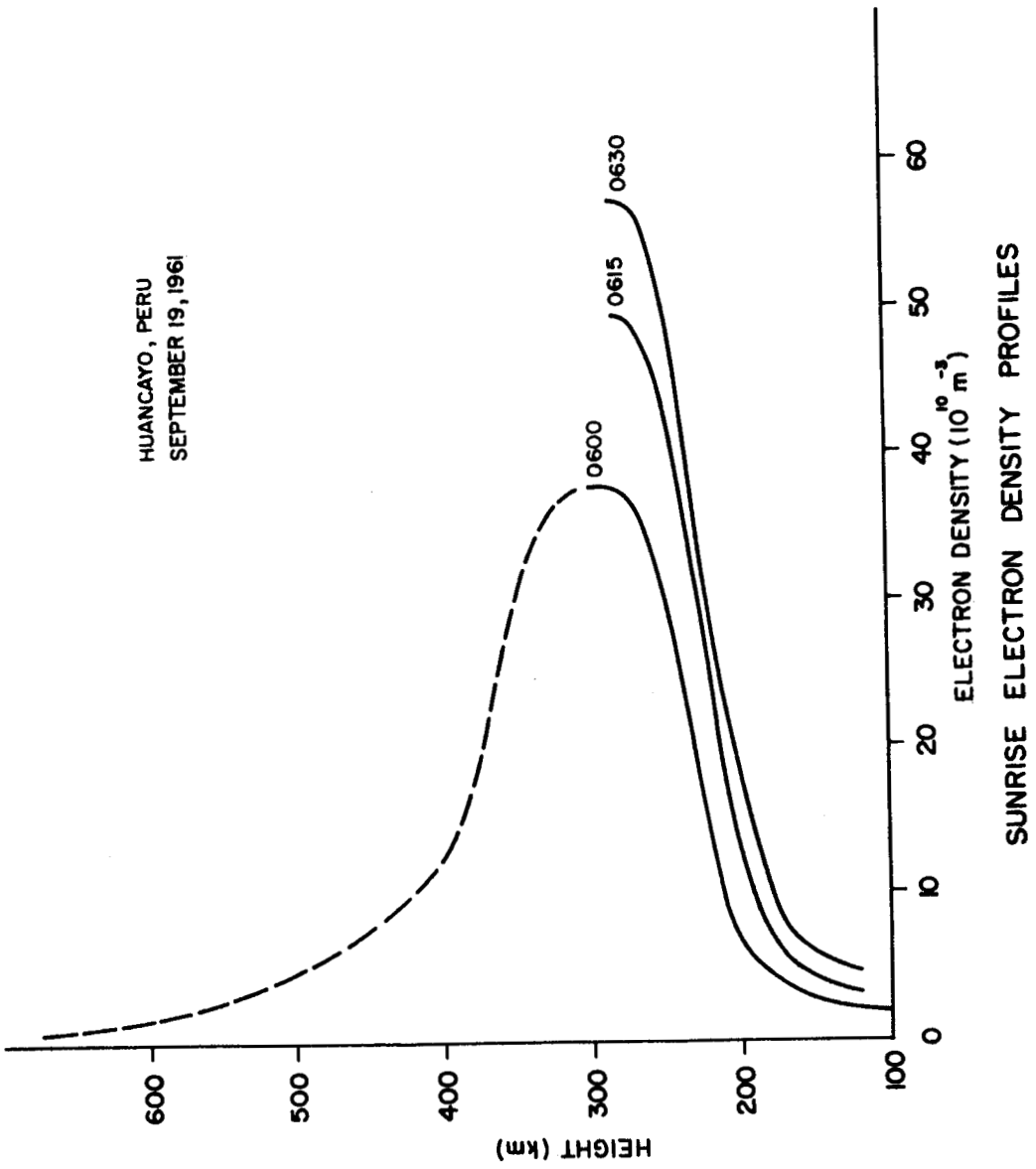

SUNRISE ELECTRON DENSITY PROFILES

FIGURE 1

smaller than supposed.

It has been suggested that this phenomenon can arise from the fact that some of the ionization in this region may be due to some minor constituents which have slow rates of recombination. While this still is an unresolved problem, it presents no serious difficulty, for we note that in the E region (approximately 100-150 km) the electron density and the production rate are small in comparison to those in the F region. Any losses occurring here will therefore be relatively small and contribute only a negligible amount to the integrated rate of change of electron density.

3.5 F-Region Losses

In the F region, however, the situation is different. Photoionization of atomic oxygen is the dominant ionization process and ionized atomic oxygen is therefore the principal ion. The major loss process in this region is then governed by the charge exchange-dissociative recombination of atomic oxygen process previously discussed. Evaluation of this loss term permits the determination of the electron loss by this mechanism. The required electron densities are readily obtained from vertical sounding electron density profiles made at the appropriate time.

Loss through the molecular nitrogen ion is also possible. It was shown by Swider (1963) that dissociative recombination was the principal loss process for this ion above about 200 km. Furthermore, under twilight conditions it is believed that quasi-photoequilibrium is followed because the lifetime of the N_2^+ ion, $1/\alpha(N_2^+)n_e$, is short. The value of $\alpha(N_2^+)$ is uncertain, but Swider's studies indicate a value of

$2 \times 10^{-7}\ (300/T)^{1.5}\ cm^3\,sec^{-1}$ and a recent laboratory value by Kasner and Biondi (1964) is $3 \times 10^{-7}\ cm^3\ sec^{-1}$ for 300 °K. This means the lifetime is on the order of 500 sec at 150 km and 25 sec at 300 km.

An alternative loss process for molecular nitrogen ions is the rapid charge transfer process

$$N_2^+ + O \rightarrow N_2 + O^+$$

which, however, does not directly affect the electron density. The rate coefficient for this process is estimated (Nicolet and Swider, 1963) to be $\geq 10^{-12}\ cm^3\,sec^{-1}$ at 150 km and $\geq 10^{-11}$ at 300 km. The lifetimes at the respective altitudes due to this mechanism are approximately 60 sec and 500 sec. Hence, molecular nitrogen ions are lost predominantly by the charge transfer process at low altitudes and by the recombination process at higher altitudes, with the transition region occurring at perhaps 200 km. This height corresponds approximately to the height of maximum N_2^+ production.

Chapter IV

Sunrise Satellite Geometry

4.1 Pictorial Description

The integrated rate of change in electron density is obtained by measuring the integrated electron density as a function of time as the satellite sweeps over the ground station. Consider a satellite such as Transit 4-A, whose ground track crosses the latitude at Huancayo, Peru at an azimuthal angle of 19 degrees. Figure 2 shows a cross sectional view of the satellite sweeping across a ground station at a height approximately 1000 km above the ground. Depicted also is an ionosphere point at a fixed height (here 300 km) and lying on the ray path between the satellite and the receiver.

It takes approximately five minutes for the satellite to pass over the ground station. However, this is not the same time period actually experienced by a point on the ray path at a given height, since it moves along with the satellite with an eastward component of velocity. Thus the ionosphere point goes through a greater local time span than does the receiving station.

A plan view of the satellite-sunrise geometry is shown in Figure 3 for the Huancayo station. Drawn to approximate scale it illustrates the location of the ionosphere point marked off in one minute intervals of the five minute satellite pass. The westward motion of the twilight line corresponding to the time in which the satellite passes over is also shown.

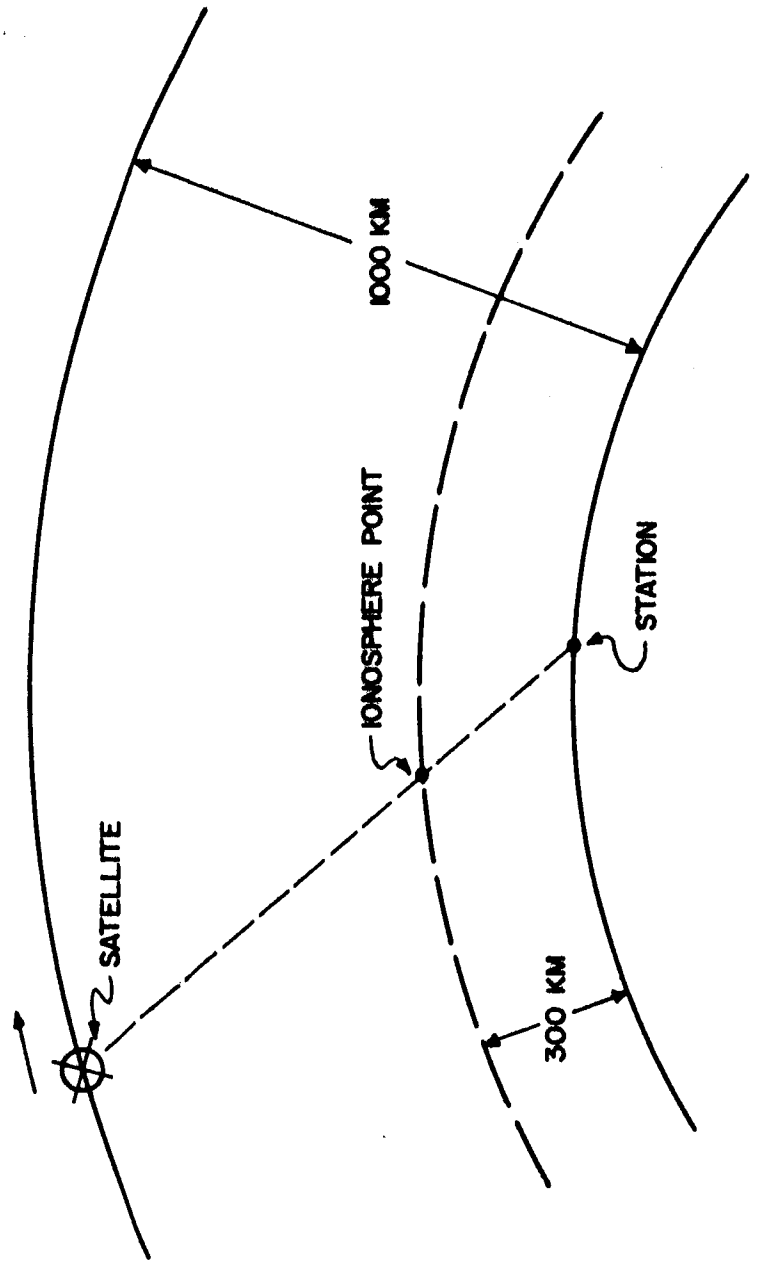

CROSS SECTION OF SUNRISE GEOMETRY

FIGURE 2

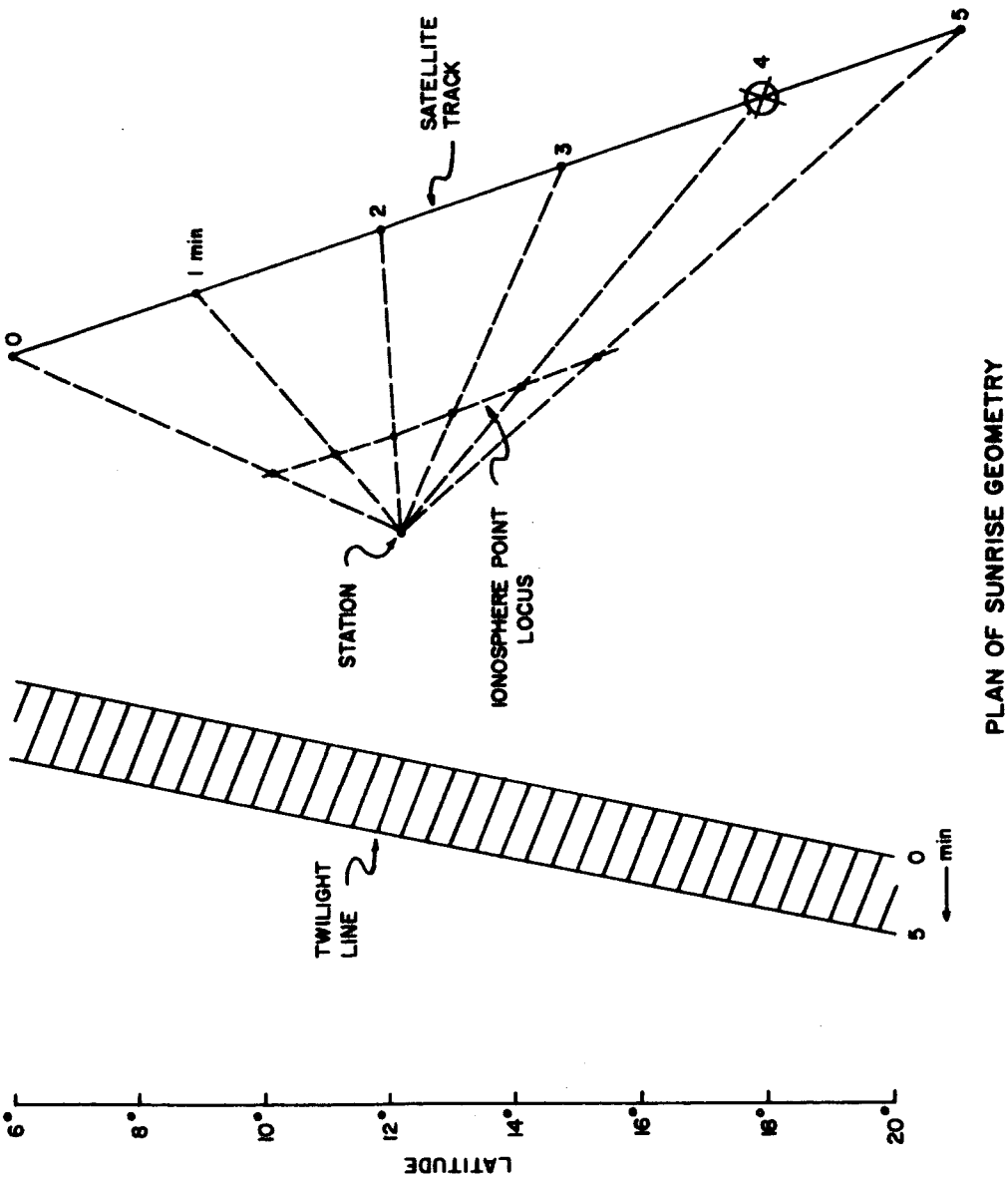

PLAN OF SUNRISE GEOMETRY

FIGURE 3

4.2 Ionosphere Time

From a knowledge of the satellite position, which is readily obtainable, and some geometry we can get the ionosphere point time corresponding to any given ground station time.

By inspection of numerous electron density profiles like that in Figure 1 it is to be concluded that the center of the region of ionization is at about 300 km. This may then be taken to be the effective height of the ionosphere. Using this height for the ionosphere point, it is found that a time of five minutes at the ground station represents a local time of approximately fifteen minutes at the ionosphere point.

4.3 Rate of Change of Electron Content

Evaluation of the integrated electron density for various satellite positions permits one to plot the total electron content as a function of the ionosphere point time and consequently determine the rate of change in electron content. Clearly, since the ionosphere point is moving, each point for which the electron density is evaluated represents a different area of the ionosphere, thus making it necessary to assume a uniformly continuous distribution of electrons in the ionosphere; that is that all areas of the ionosphere have the same electron density distribution for a given local time. This, it is believed, is a reasonable assumption, particularly if enough production has occurred to override the effects of any non-uniform distribution of residual ionization. Furthermore, any major deviation from this condition should appear in the records and thus make them useless. An example of this will be seen later.

Chapter V

Theoretical Considerations

5.1 Increase in Electron Content Due to Production

Several features of the production as determined by theory are noteworthy. Using the relation

$$q_T = \frac{\gamma I_\infty}{Ch(H, \chi)}$$

and supplying the variables with representative values one can determine the relative electron content (neglecting losses) due to production occurring at the theoretical rate as χ increases, i.e., as the sun rises. This has been done and the results are shown in Figure 4, where an arbitrary zero level of electron content is used. The most important feature of this curve is that it is convex upwards; however, over a fifteen minute interval, say centered around sixteen minutes after ground sunrise ($\chi = 86°$), the increase in electron content is quite linear. In fact, when electron loss is taken into consideration it would be expected to be even more linear since the loss rate increases with an increase in electron density. With this in mind a linear fit of the experimental data is made, since it corresponds approximately to a fifteen minute time interval.

5.2 Production and Scale Height Dependence

The production rate is dependent upon scale height through the Chapman function and consequently, the dependence of the Chapman function itself upon scale height is important. In Figure 5 the Chapman function is plotted as a function of scale height for various values of

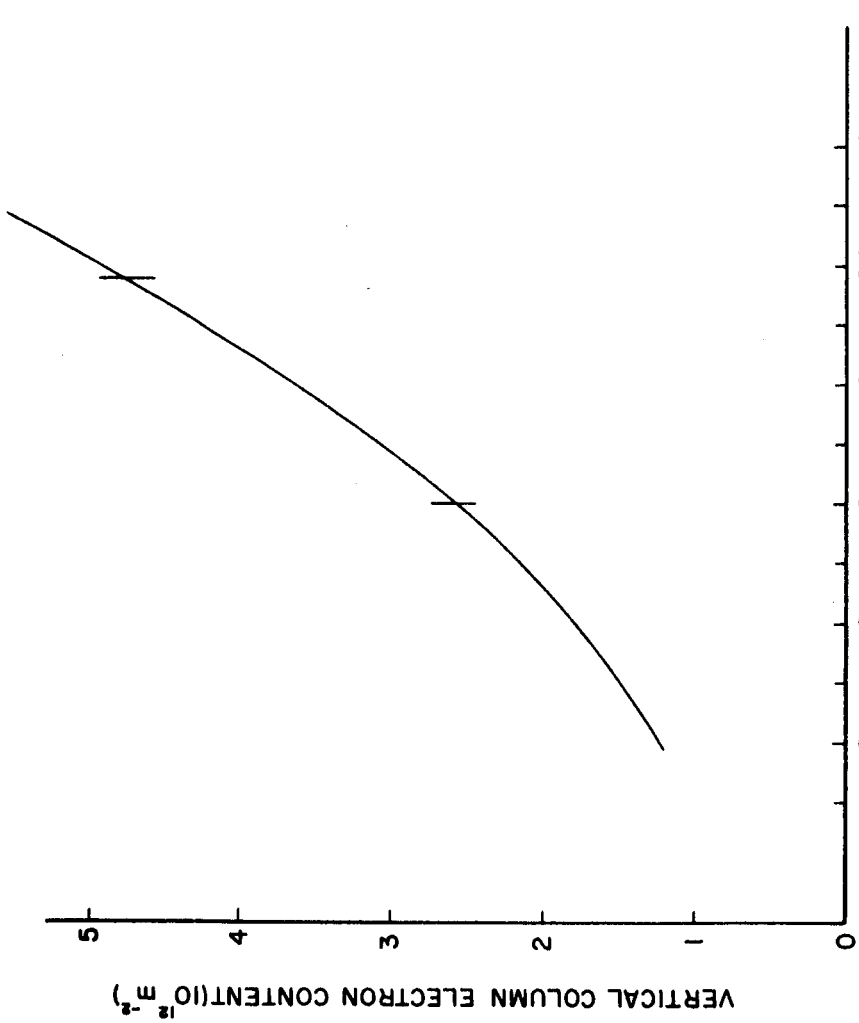

VERTICAL COLUMN ELECTRON CONTENT CALCULATED FROM $q = \frac{\gamma I_\bullet}{Ch(H,\chi)}$

FIGURE 4

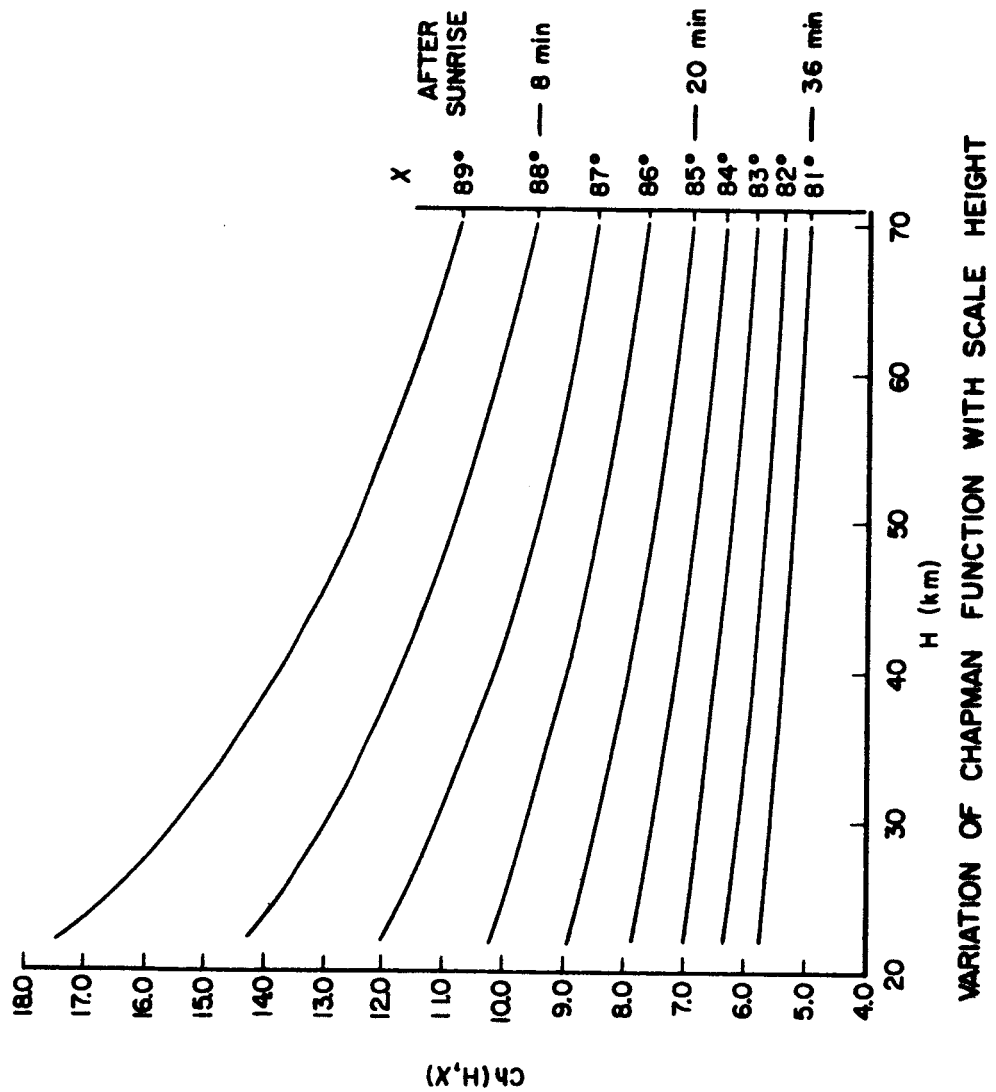

VARIATION OF CHAPMAN FUNCTION WITH SCALE HEIGHT

FIGURE 5

solar zenith angle. One notes that the function is less sensitive to scale height for smaller zenith angles. However, even at 88° over the scale height range of most interest (25-50 km) it varies from a mean only by about 15%.

From this we conclude that times further from sunrise would be more desirable in that the function is less sensitive to scale height. Also, as mentioned earlier, the use of times further from sunrise minimizes the effects of a non-uniform distribution of residual ionization. However, at later times the loss rate becomes greater and the uncertainties therein become more significant. Consequently, a compromise must be made, if possible. In view of this, times around fifteen to twenty minutes after ground sunrise appear most favorable for this study.

5.3 Effective Scale Height

Before using the Chapman function it remains to determine the effective scale height. At the present time there is still some uncertainty as to what the appropriate scale height is. It has been found by Ratcliffe, Schmerling, Setty and Thomas (1956) to be about 45 km, which appears reasonable when we remember that the scale height of atomic oxygen, the principal constituent, is between 35 and 50 km in the 180 to 500 km height range. However, as these workers are quick to admit, their estimation is subject to considerable uncertainty. It seems reasonable to assume that the minimum value would be that of molecular nitrogen and the maximum value would be approximately that of atomic oxygen. Consequently, we would expect the scale height to lie in the 25 to 50 km range.

5.4 Model Study of Production

Two semi-independent methods of determining the effective scale height from a model, which will also be of general interest, will now be considered. Using a model atmosphere and assumed solar flux intensities, production rates for various solar elevations will be calculated.

An indication of solar activity is given by the intensity of the 10.7 cm solar radiation flux which varies during the eleven year solar cycle from a minimum of S = 70 to a maximum of S = 250, where S is measured in 10^{-22} watts/m^2 - cps. For the period of our experimental data, 1961-1963, the sun was fairly quiet and the value of S was approximately 100.

The atmospheric model chosen is one of Nicolet's recent ones for an 800°K thermosphere, which corresponds to the thermospheric temperature around sunrise for S = 100. This model is quite comparable to Harris and Priester, (1962) S = 100, 6 A.M. model. The densities of O_2 and N_2 differ generally by less than a factor of 1.3, being greater in Nicolet's model except below approximately 220 km. The agreement for atomic oxygen densities is much better, differing generally by less than a factor of 1.1.

Use was made of a computer program, prepared by Mr. Peter Banks of this Laboratory, of the equation given in Chapter II for electron production due to chromatic radiation being absorbed by a multiconstituent atmosphere. The three principal absorbers, atomic oxygen, molecular oxygen and molecular nitrogen were considered. Hinteregger, Hall and Schmidtke (1964) obtained solar fluxes for 71

wavelengths or wavelength ranges in the 1027-10A interval and also gave total and ionization cross sections for the corresponding wavelength or wavelength interval. These fluxes were to be representative of those for July 1963 and since S = 100 for that period it is assumed that they are also representative of our period of interest.

The resulting production rates for each of the constituents are shown in Figures 6 and 7 for χ equal to 83 and 88 degrees, respectively.

It is interesting to note that the total production ratios $O:O_2:N_2$ are approximately 3:1:2.3 for $\chi = 83°$ and 10:2:5 for $\chi = 88°$. Thus the production due to molecular oxygen represents only about one-seventh of the total.

The temperatures and scale heights for each absorber which are representative of those used in the model are tabulated in Table I. The scale heights computed from the Harris and Priester model are also given for comparison.

5.5 Effective Scale Height Determined from Model

Since a very complex ionization and absorption process is being greatly simplified, a non-rigorous determination of the scale height for the "equivalent single constituent atmosphere" must be made.

It is assumed that for the three constituent case the effective scale height to be used in the Chapman production function for integrated production may be determined to a good approximation by finding the mean scale height weighted according to production.

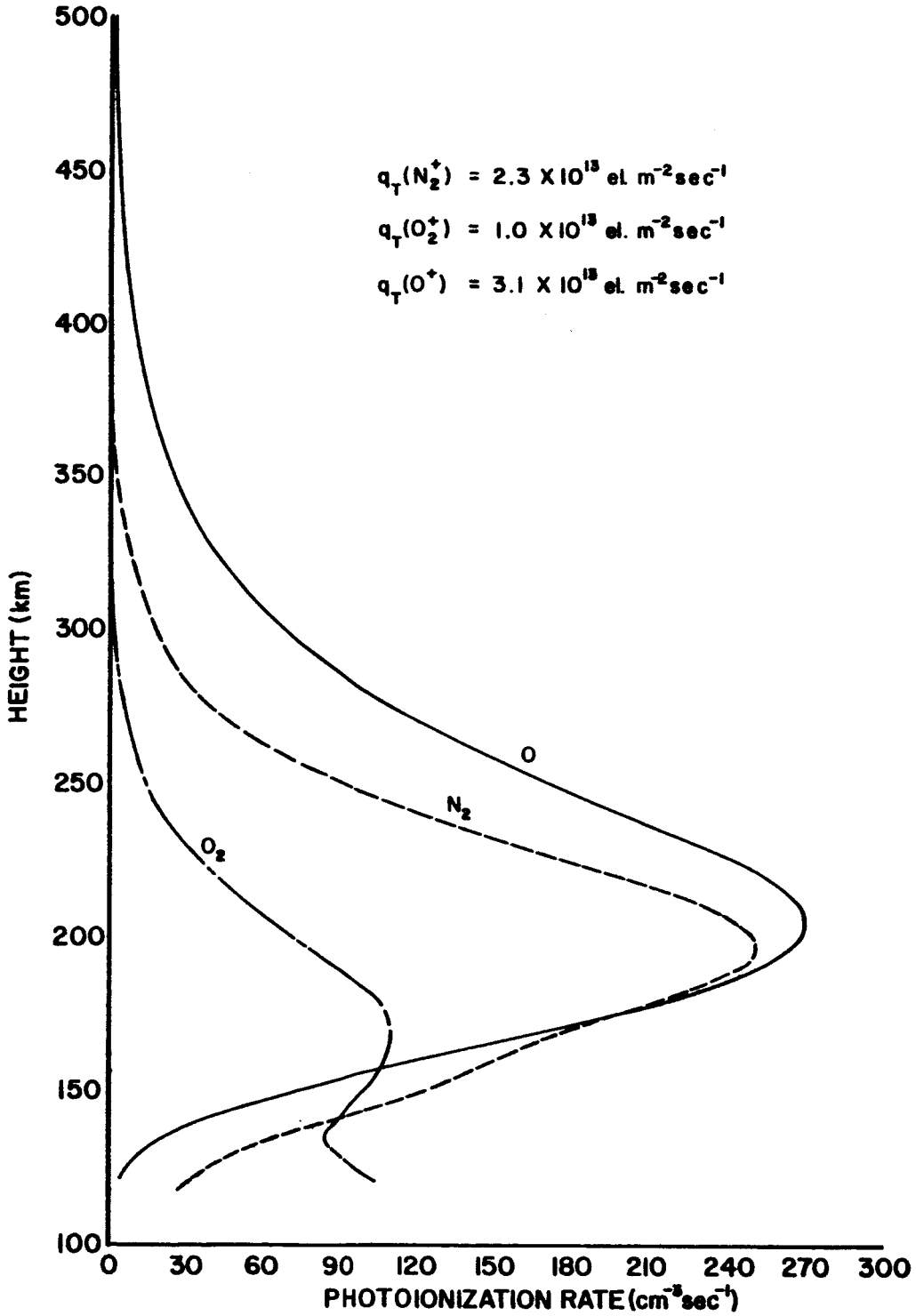

PRODUCTION FOR $\chi = 83°$

FIGURE 6

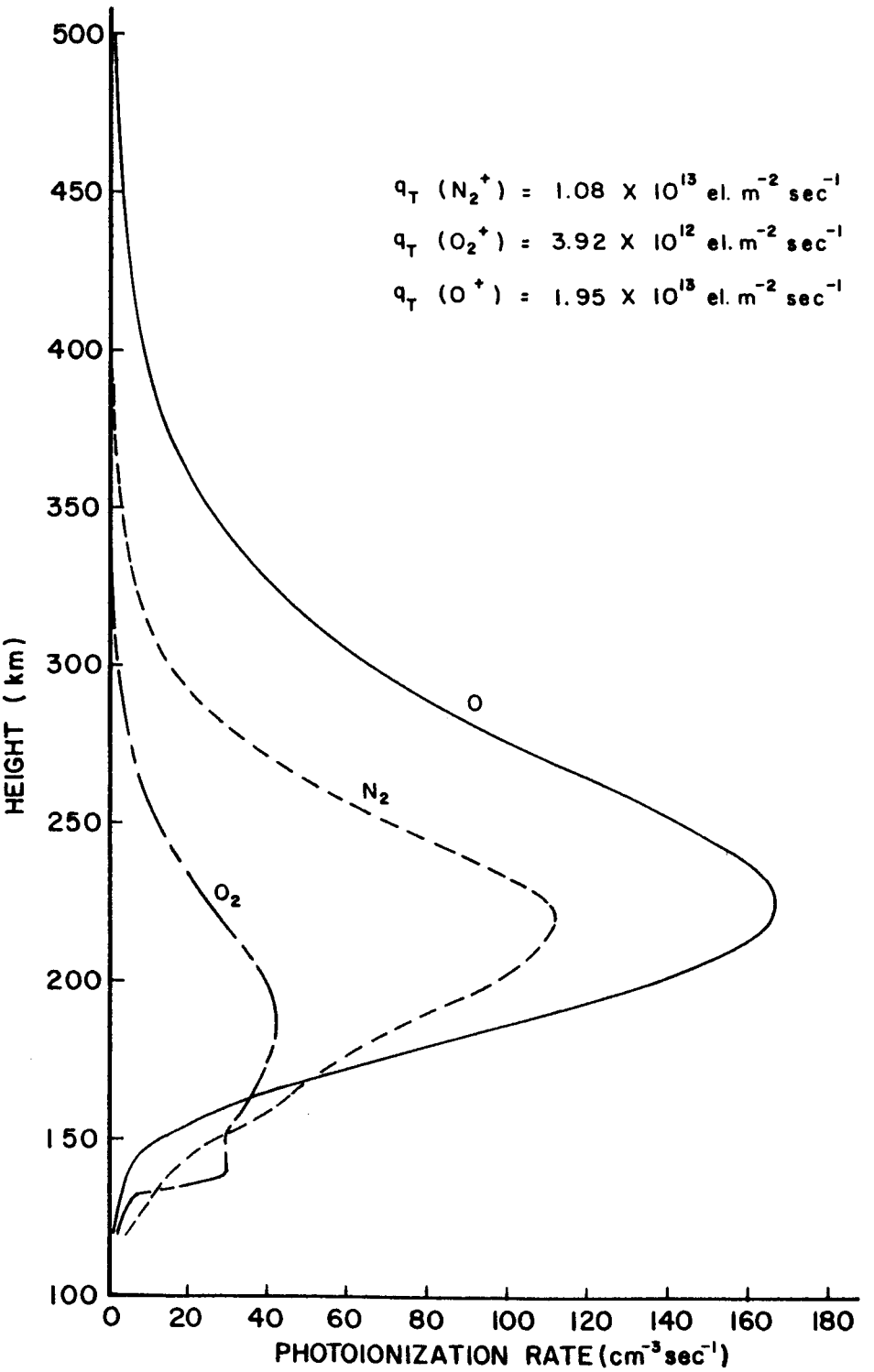

PRODUCTION FOR $\chi = 88°$

FIGURE 7

Table I

Model Scale Heights and Temperatures

Height (km)	Temperature (°K)		H(O) (km)		$H(O_2)$ (km)		$H(N_2)$ (km)	
	H&P	Nicolet	H&P	Nicolet	H&P	Nicolet	H&P	Nicolet
120	355	291	19.2	16.0	9.59	8.0	11.2	9.2
160	560	627	30.6	34.9	15.3	17.5	17.9	19.9
200	665	753	36.7	42.5	18.4	21.2	21.5	24.3
240	730	785	40.8	44.8	20.4	22.4	23.8	25.6
300	777	796	44.4	46.3	22.2	23.1	25.9	26.4
400	801	799	47.3	47.9	23.7	23.9	27.6	27.4

Thus, let H_m be the mean scale height at a given altitude, given as

$$H_m = \frac{\Sigma H(Y)q(Y)}{\Sigma q(Y)} ,$$

where Y represents a particular absorber. Then the production weighted mean of H_m is given as

$$\overline{H}_m = \frac{\int q\, H_m\, dh}{\int q\, dh} .$$

We find that for $\chi = 83°$ $\overline{H}_m = 30.1$ km and for $\chi = 88°$ $\overline{H}_m = 25.6$ km. These results are not too surprising when we note that at 200 km, where production in this model is maximum, the respective scale heights are 37, 18 and 21 km.

Furthermore, note that the equation

$$q_T = \frac{\gamma I_\infty}{Ch(H, \chi)}$$

contains two unknowns, γ and H, when the total production, incident flux and solar zenith angle are known. We thus have a method of determining a time average effective scale height, since for our model the required three quantities are known. Therefore, by solving the equation simultaneously for χ equal to 83° and 88° we can determine γ and H. We find that if the effective ionosphere height is taken as 300 km the effective scale height is 30.2 km, whereas, if it is taken at 200 km the scale height is 29.9 km. Clearly, these results agree very well with the upper limit of that determined by the first

method, and also show that the result obtained by the latter method is quite independent of where the effective ionosphere height is taken.

It is to be concluded that for an 800 °K thermosphere the effective scale height is of the order of 30 km for the three absorber cases. While it is true that in general (see Table I) the scale heights of the Nicolet model are somewhat larger than those of the Harris and Priester model, due to a less rapid decrease in temperature with decreasing altitude, it is unlikely that the scale height would ever exceed 35 km or be less than 25 km. In this range a 5 km uncertainty at $\chi = 88°$, where the change in the Chapman function is almost maximum, the uncertainty in that function is only 6%. Consequently, for the conditions of our experimental data, S = 100, we can be quite confident of our results if we use 30 km for the effective scale height. Clearly, for much different thermospheric temperatures corresponding to other S values the effective scale height will not necessarily be the same and should be re-determined for those conditions.

5.6 Ionizing Efficiency

An interesting by-product of the second method is that the ionizing efficiency is 66% for this particular model. This simply reflects the cross sections and intensity distributions used in the model, that is, an average thereof. This result should consequently be used with caution in that it relies on the accuracy of two somewhat dubious quantities; nevertheless, it does give some indication of what the effective ionizing efficiency might be. Knowledge of this quantity is not essential, however, unless one wishes to know the total rather than the ionizing flux, which is quite informative in itself. No

attempt to determine this quantity will be made here, it rather will be assumed to be unity, i.e., 100% efficient.

Should the N_2^+ ions be in quasi-photoequilibrium, as suggested earlier, there will be no observable change of electron content due to ionization of molecular nitrogen. From this model we note that the "equivalent" ionization efficiency factor would be about 43% rather than 66%. That is, the total photon flux in the 10 to 1027A range would be 46 to 56% (χ equals 88° to 83°) larger than calculated assuming that all ion production (including N_2^+) is being measured.

Chapter VI

Experimental Data

6.1 Source of Data

The technique we just developed was applied to experimental data from Transit 4-A taken at Huancayo, Peru, covering the period of 1961 to 1963. Due to orbital precession one normally can only obtain sunrise records for one day and at best three successive days in about every six weeks. Consequently, records available for Transit 4-A are severely limited; however, seven records satisfactory for the sunrise measurements were found. There are two sets of records for three successive days in September 1961 and July 1962, and another record for February 1963, thus permitting an examination of a variety of conditions.

As was indicated in Chapter IV and evidenced in Figure 1, the effective ionosphere height was taken as 300 km for purposes of determining integrated electron content and ionizing flux intensities.

6.2 Loss Calculations

Electron densities for loss calculations were obtained from vertical sounding profiles, such as in Figure 1, made at times of satellite passage. The loss due to atomic oxygen was calculated from

$$L = \frac{\alpha \beta n^2}{\alpha n + \beta} \quad .$$

It is assumed that conditions are sufficiently close to those of nighttime that recombination coefficients determined at night are

applicable. Quinn (1964) studied the nighttime ionosphere at six stations (including Puerto Rico) and suggested that the recombination coefficient exhibits no latitude dependence. He also suggests that there is a seasonal variation and lists values of the coefficient appropriate to the various conditions. To allow for uncertainties in the coefficients loss rates were calculated for several values and combinations of the coefficients.

A typical loss rate profile is shown in Figure 8 and represents values of the coefficients which were considered most appropriate for prevailing conditions. The quadratic loss coefficient, α was taken as 10^{-14} m^3 sec^{-1} and the linear loss coefficient, β, was taken to be $0.25 \times 10^{-4} \exp - \left(\frac{h - 300}{H}\right)$ sec^{-1}, where H = 20 km. The important thing to note is that in this profile, as well as in the others, the loss rate above the F maximum at about 300 km is negligible. Consequently, the vertical sounding profiles are perfectly adequate without extrapolation above the F maximum for providing electron densities used in the loss rate calculations.

Integrated loss rates, L_T, for each of the records and for various loss coefficients are tabulated in Table II. The total loss rates are seen to be mostly dependent upon the linear loss coefficient. The maximum values (b) are approximately eight times the minimum in (d) for fairly extreme values of the coefficients. The most probable total loss rates (g) are generally three and one half times the minimum (d). It furthermore is found that the total loss rate is only slightly influenced by a change in scale height. A reasonably good estimate of the loss rate due to this mechanism is thus obtained.

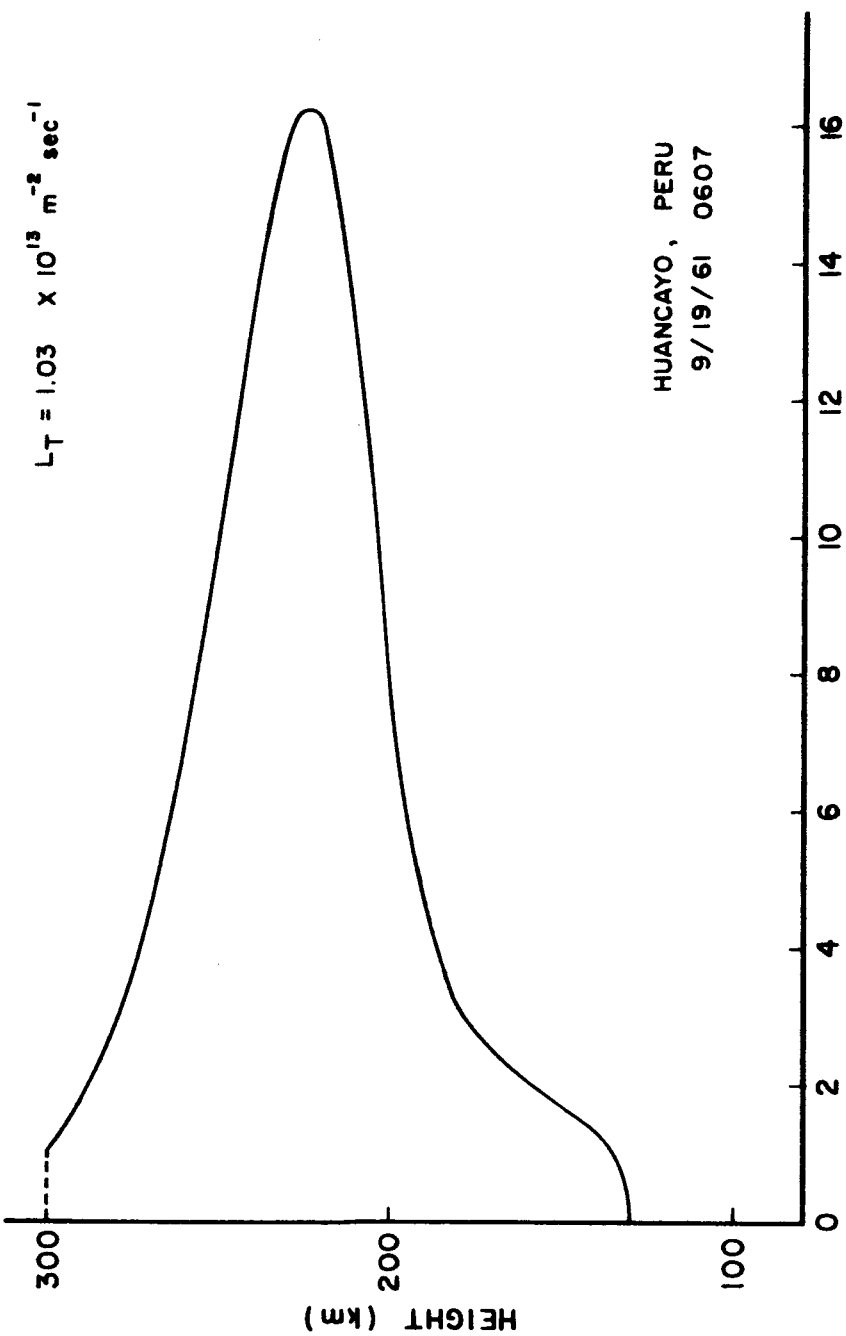
LOSS RATE PROFILE
HUANCAYO, PERU
9/19/61 0607
L_T = 1.03 X 10^{13} m^{-2} sec^{-1}
HEIGHT (km)
300
200
100
0
2
4
6
8
10
12
14
16
LOSS RATE (10^{-7} m^{-3} sec^{-1})

FIGURE 8

Table II

Integrated Atomic Oxygen Loss Rates

Ident.	α $\times 10^{-14}$	β $\times \exp -(\frac{z-300}{20})$	$L_T \times 10^{13}$ el m^{-2} sec^{-1} 9/18/61	9/19/61	7/27/62	7/28/62	7/29/62	2/25/63
a	0.5	10^{-5}	0.23	0.46	0.16	0.33	0.29	0.66
b	0.5	6.5×10^{-4}	1.3	3.6	0.58	1.6	0.89	3.0
c	0.5	2×10^{-4}	0.92	2.4	0.46	1.1	0.69	2.3
d	0.2	10^{-5}	0.15	0.32	0.092	0.20	0.16	0.42
e	10	10^{-5}	0.96	1.3	0.70	1.4	0.16	2.3
f	2	10^{-5}	0.45	0.74	0.32	0.66	0.66	1.2
g	1	0.25×10^{-4}	0.52	1.0	0.35	0.71	0.61	1.5

6.3 Rate of Change of Electron Content and Data Analysis

The rate of change of electron content was determined by evaluating the integrated electron content, with B_L sec χ' taken at 300 km, and plotting it as a function of local mean time. The results for each of the seven records are shown in Figures 9-15. The quasi-transverse point, that is, the point where propagation is perpendicular to the magnetic field, occurs near the center of the record. It was found that data points a couple of minutes on either side of the quasi-transverse point were strongly influenced by its exact location. Because orbital data only allowed determining the quasi-transverse time to within two seconds, discontinuous curves frequently resulted. An illustration of this is shown in Figure 16. It was assumed that the electron content was a continuous function of time and so the quasi-transverse time was adjusted to give reasonably continuous curves. It is believed that this phenomenon has previously been neglected.

The plot of integrated electron content versus ionosphere mean time shown in Figure 9 is a good illustration of the results obtained for a non-uniformly continuous horizontal electron distribution. This record was characterized by considerable scintillation indicating irregularities in the ionosphere. The ionograms made during this period exhibited spread F, also indicating irregularities. As a result, the electron content versus time curve is not monotonic. Actually, it is not a matter of time, but rather the area of the ionosphere being viewed, since these two factors are superimposed upon each other, with the latter factor dominating in this case. Because

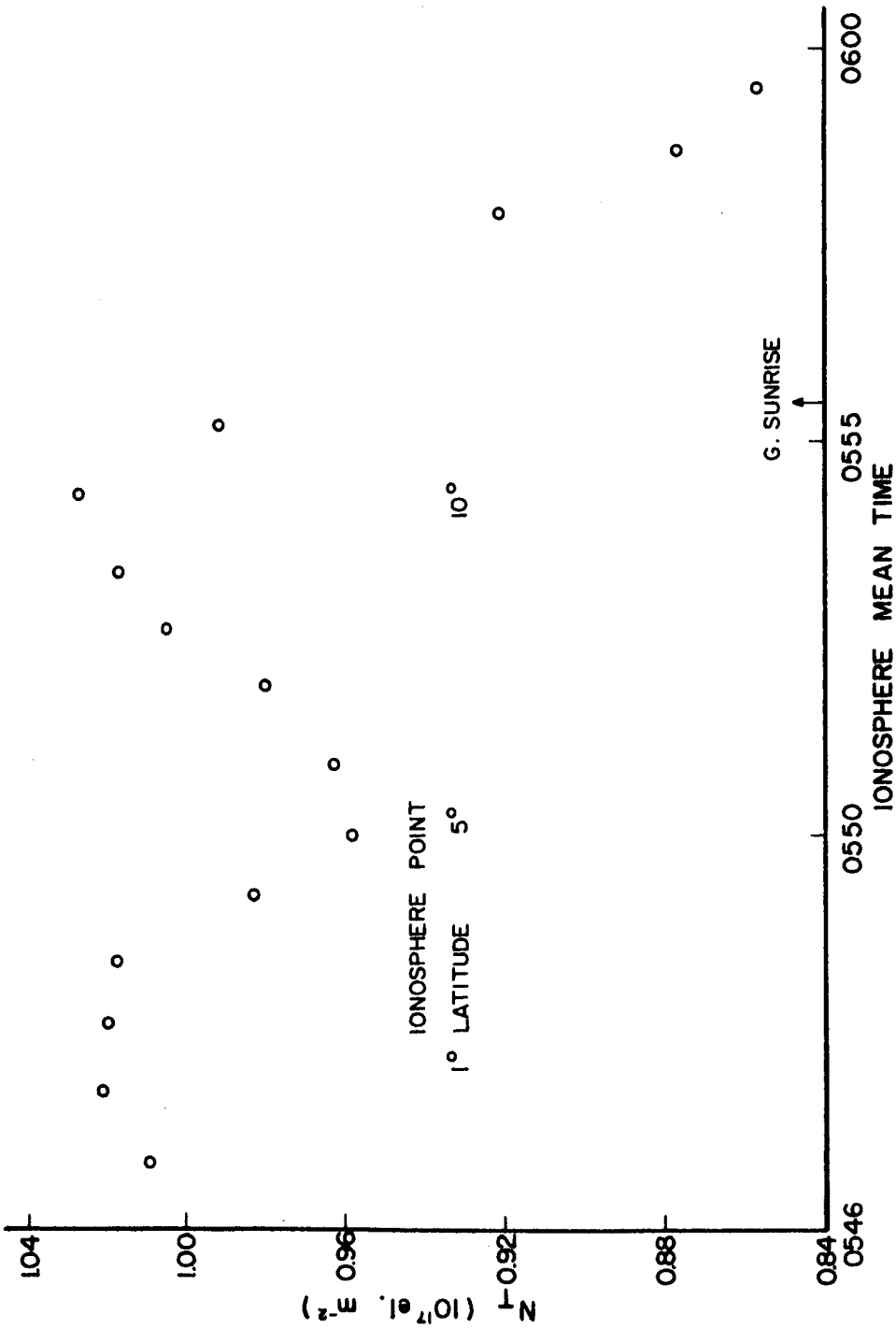
1.04
1.00
0.96
0.92
0.88
0.84
N_T (10^{17} el. m^{-2})
0546
0550
0555
0600
G. SUNRISE
IONOSPHERE MEAN TIME
N_T VERSUS TIME 9-18-61
IONOSPHERE POINT
1° LATITUDE
5°
10°

FIGURE 9

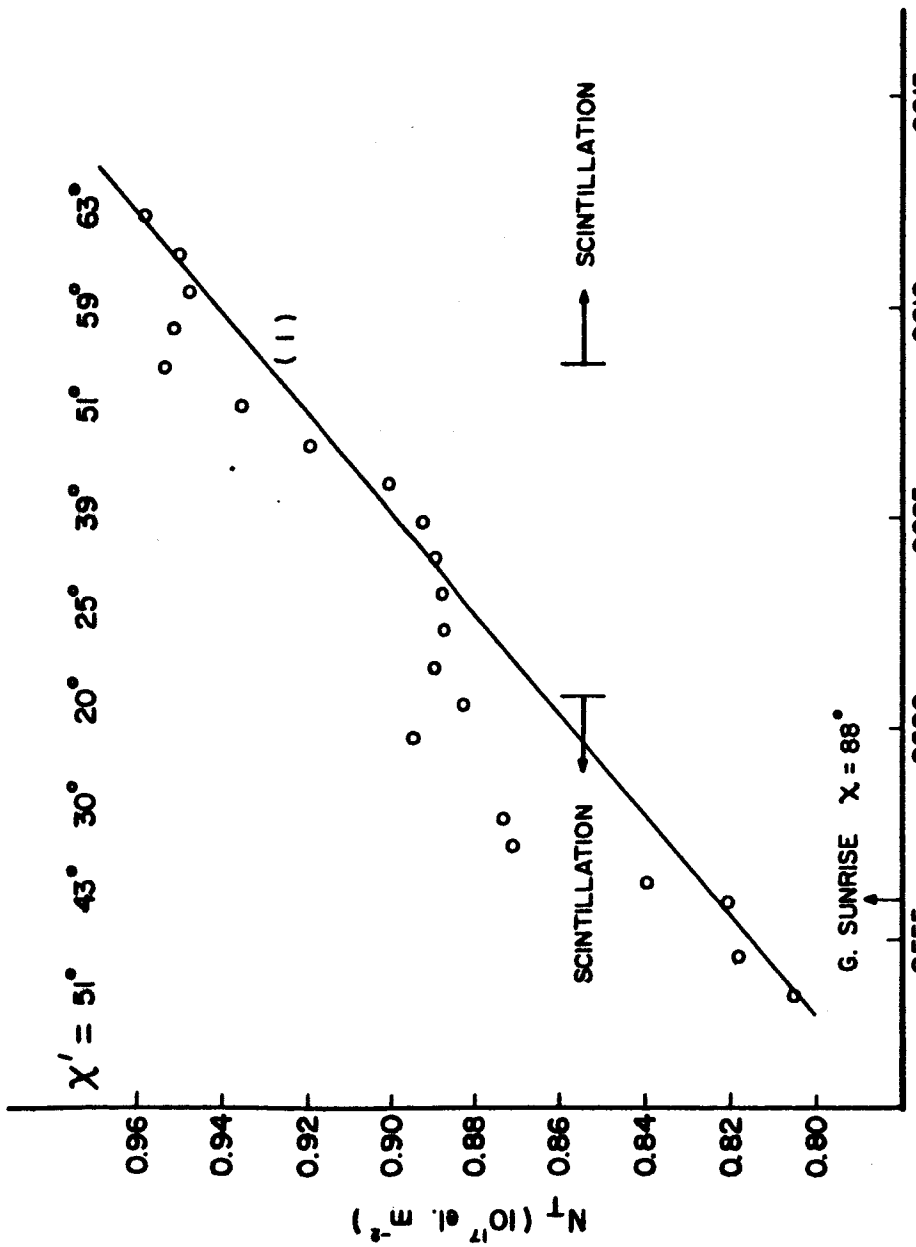
χ' = 51° 43° 30° 20° 25° 39° 51° 59° 63°
(1)
SCINTILLATION
SCINTILLATION
G. SUNRISE χ = 88°
0555
0600
0605
0610
0615
IONOSPHERE MEAN TIME
N_T VERSUS TIME 9-18-61
N_T (10^{17} el. m^{-2})
0.96
0.94
0.92
0.90
0.88
0.86
0.84
0.82
0.80

FIGURE 10

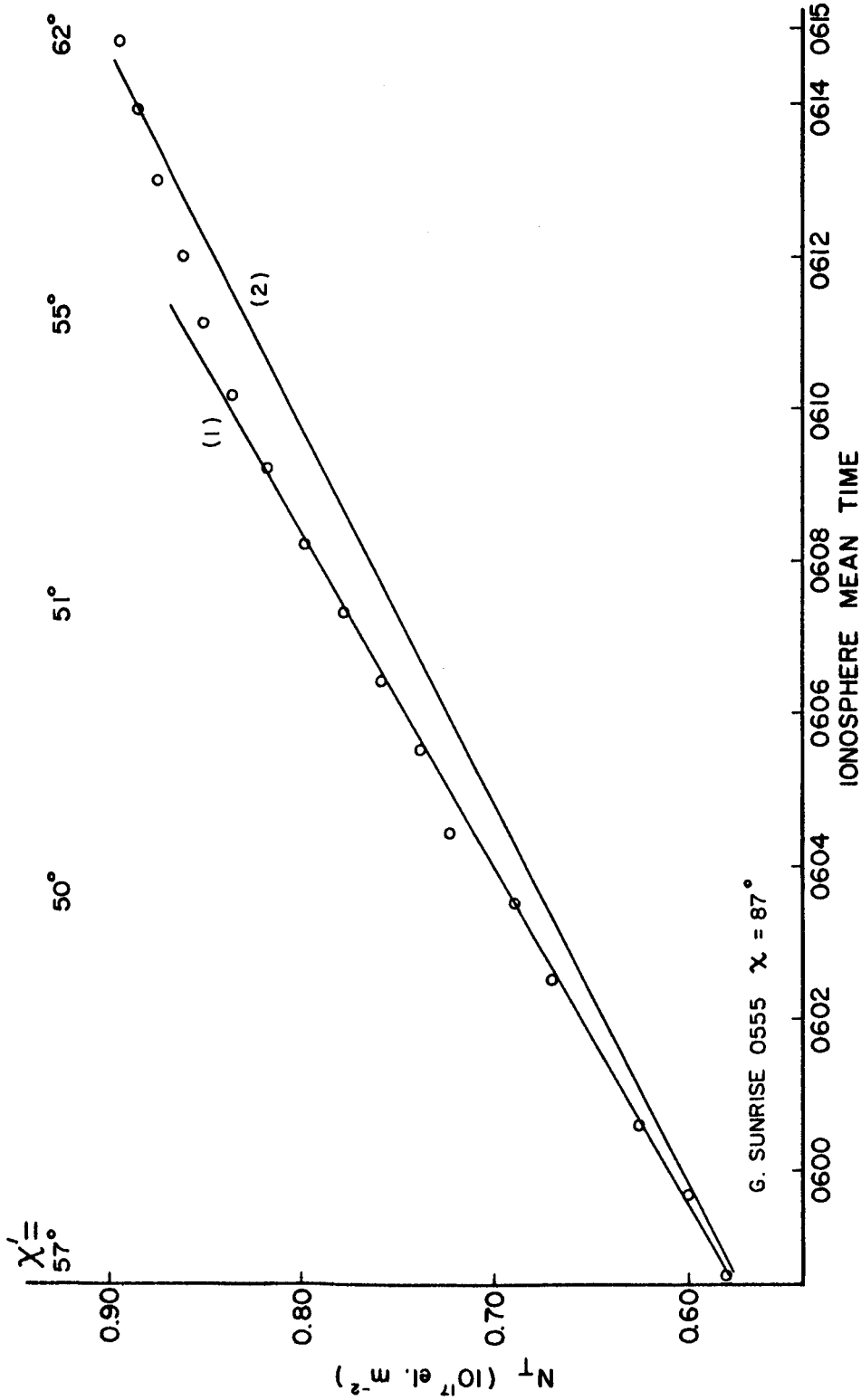
N_T VERSUS TIME 9-19-61
IONOSPHERE MEAN TIME
G. SUNRISE 0555 χ = 87°
(1)
(2)
χ' = 57°
50°
51°
55°
62°
0600
0602
0604
0606
0608
0610
0612
0614
0615
0.60
0.70
0.80
0.90
N_T (10^{17} el. m^{-2})

FIGURE 11

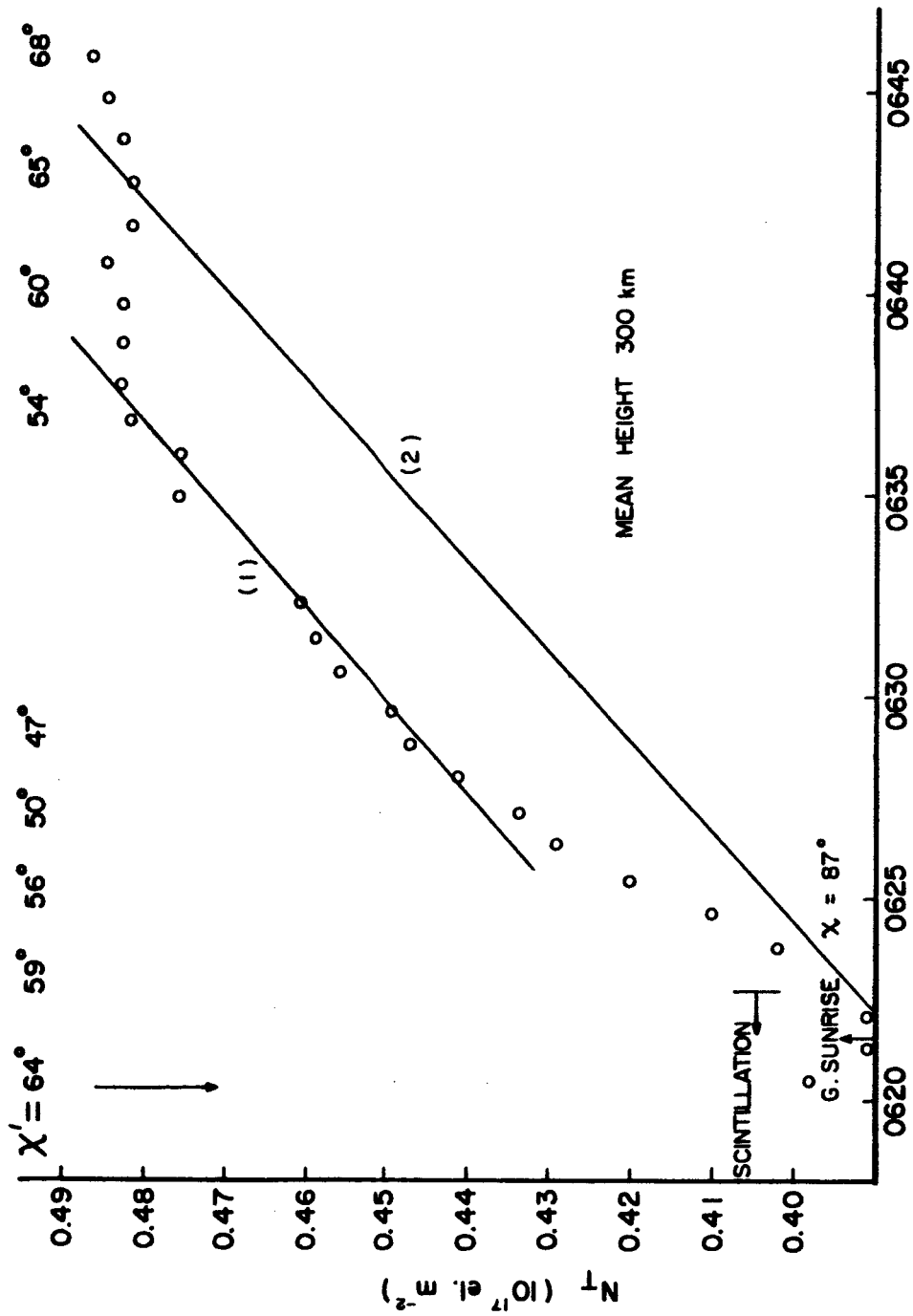

N_T VERSUS TIME 7-27-62

FIGURE 12

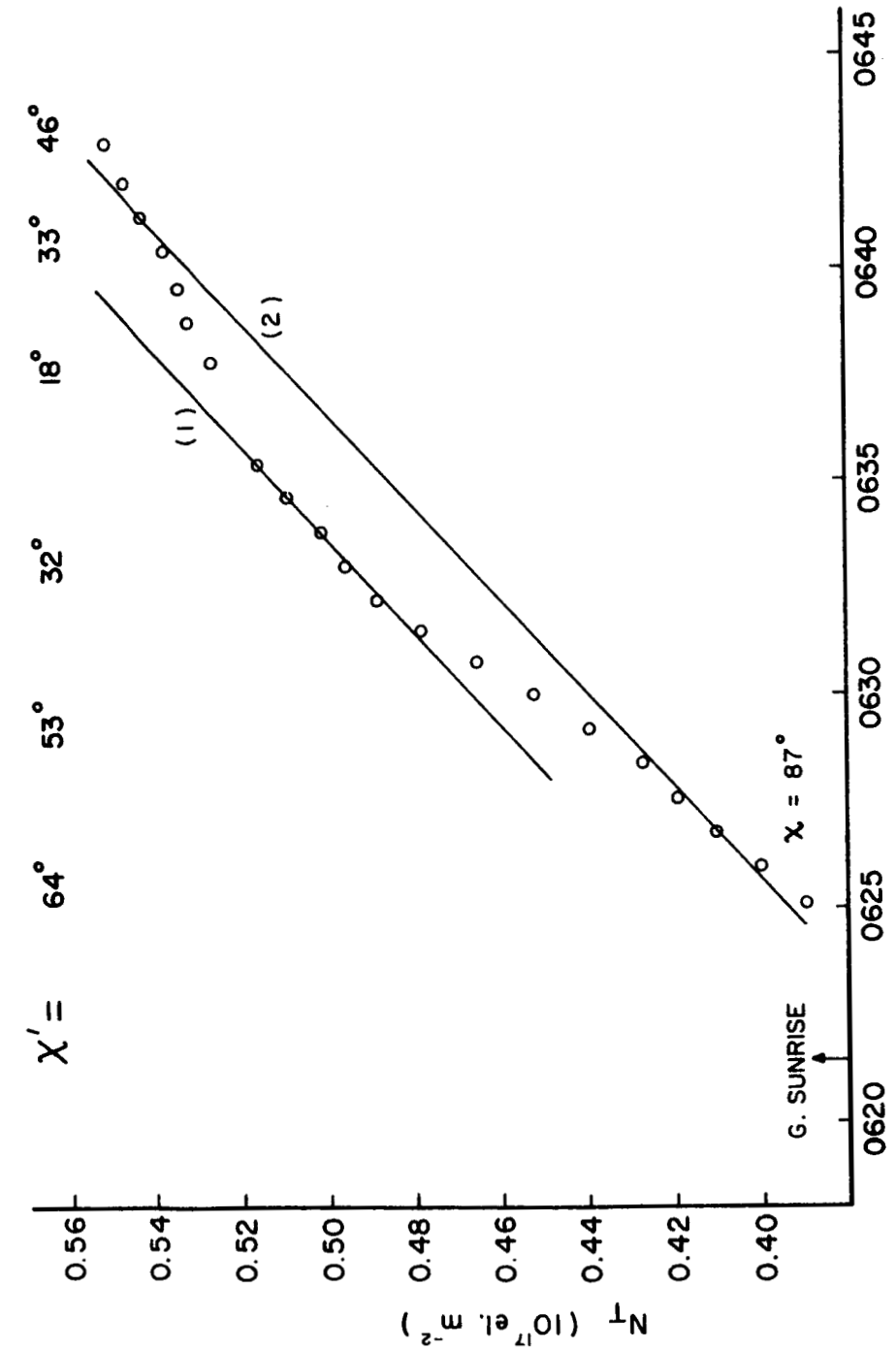
χ' = 64° 53° 32° 18° 33° 46°
(1)
(2)
χ = 87°
G. SUNRISE
0620
0625
0630
0635
0640
0645
IONOSPHERE MEAN TIME
N_T VERSUS TIME 7-28-62
N_T (10^{17} el. m^{-2})
0.40
0.42
0.44
0.46
0.48
0.50
0.52
0.54
0.56

FIGURE 13

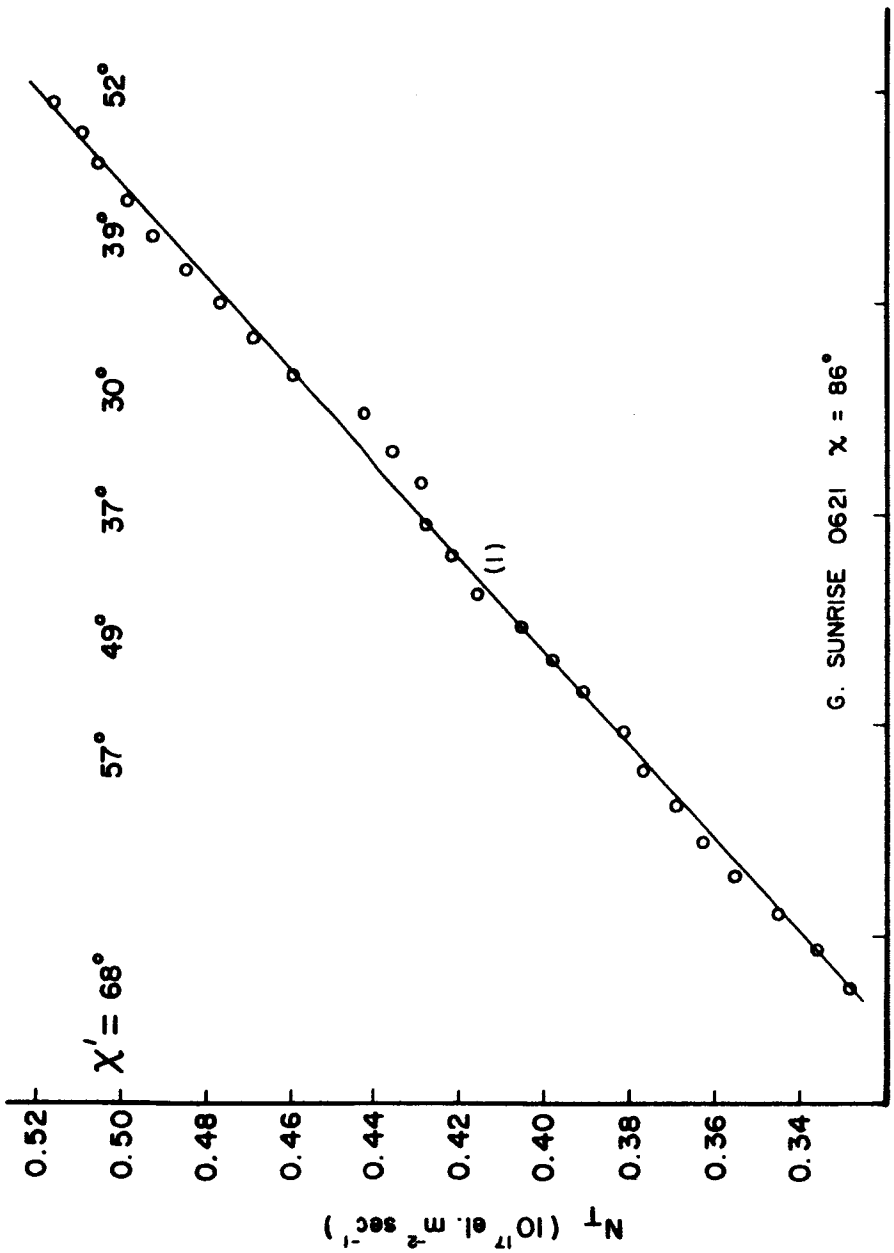

N_T VERSUS TIME 7-29-62

FIGURE 14

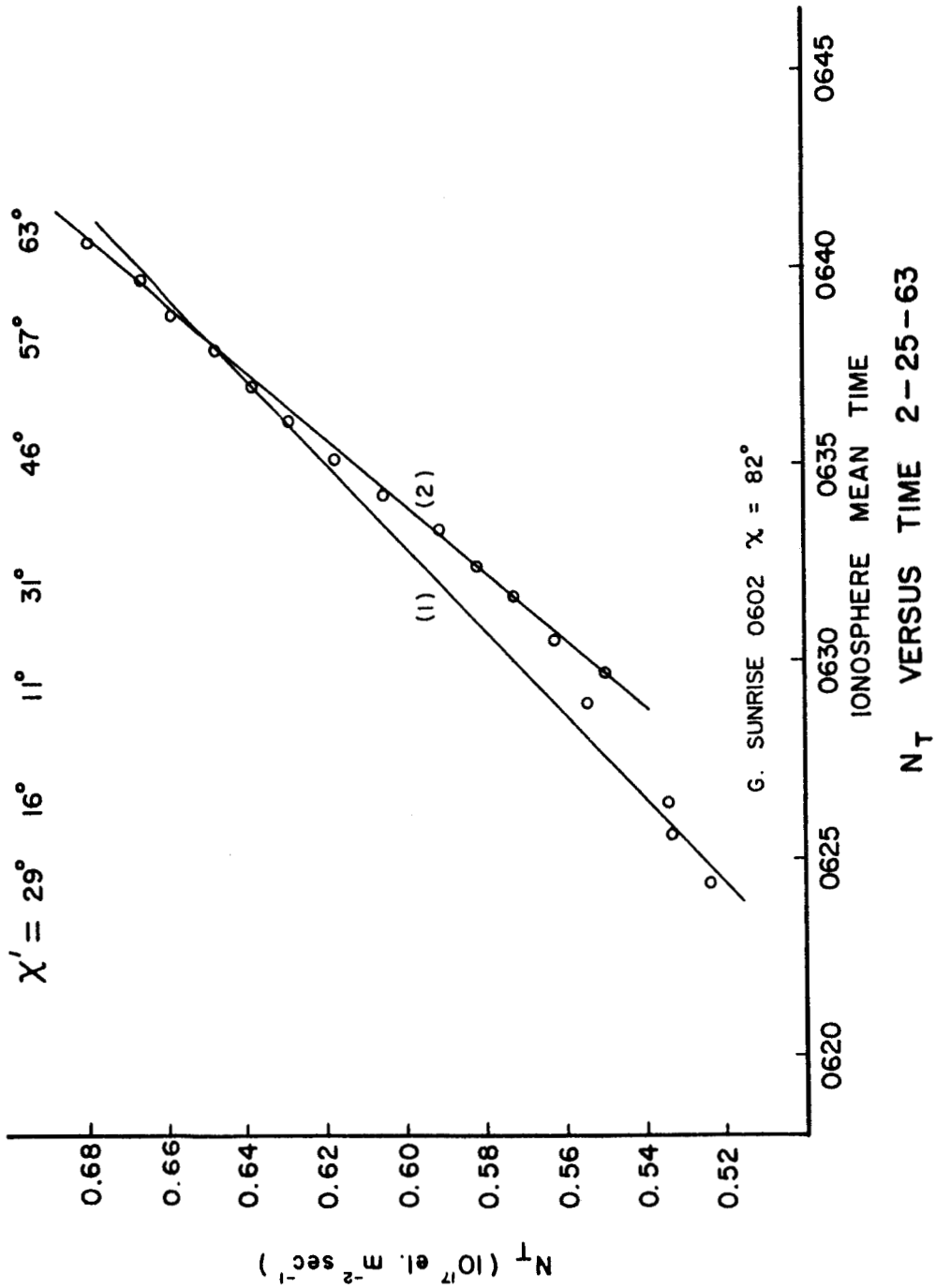
χ' = 29° 16° 11° 31° 46° 57° 63°
(1)
(2)
G. SUNRISE 0602 χ = 82°
0620
0625
0630
0635
0640
0645
IONOSPHERE MEAN TIME
N_T VERSUS TIME 2-25-63
N_T (10^17 el. m^-2 sec^-1)
0.68
0.66
0.64
0.62
0.60
0.58
0.56
0.54
0.52

FIGURE 15

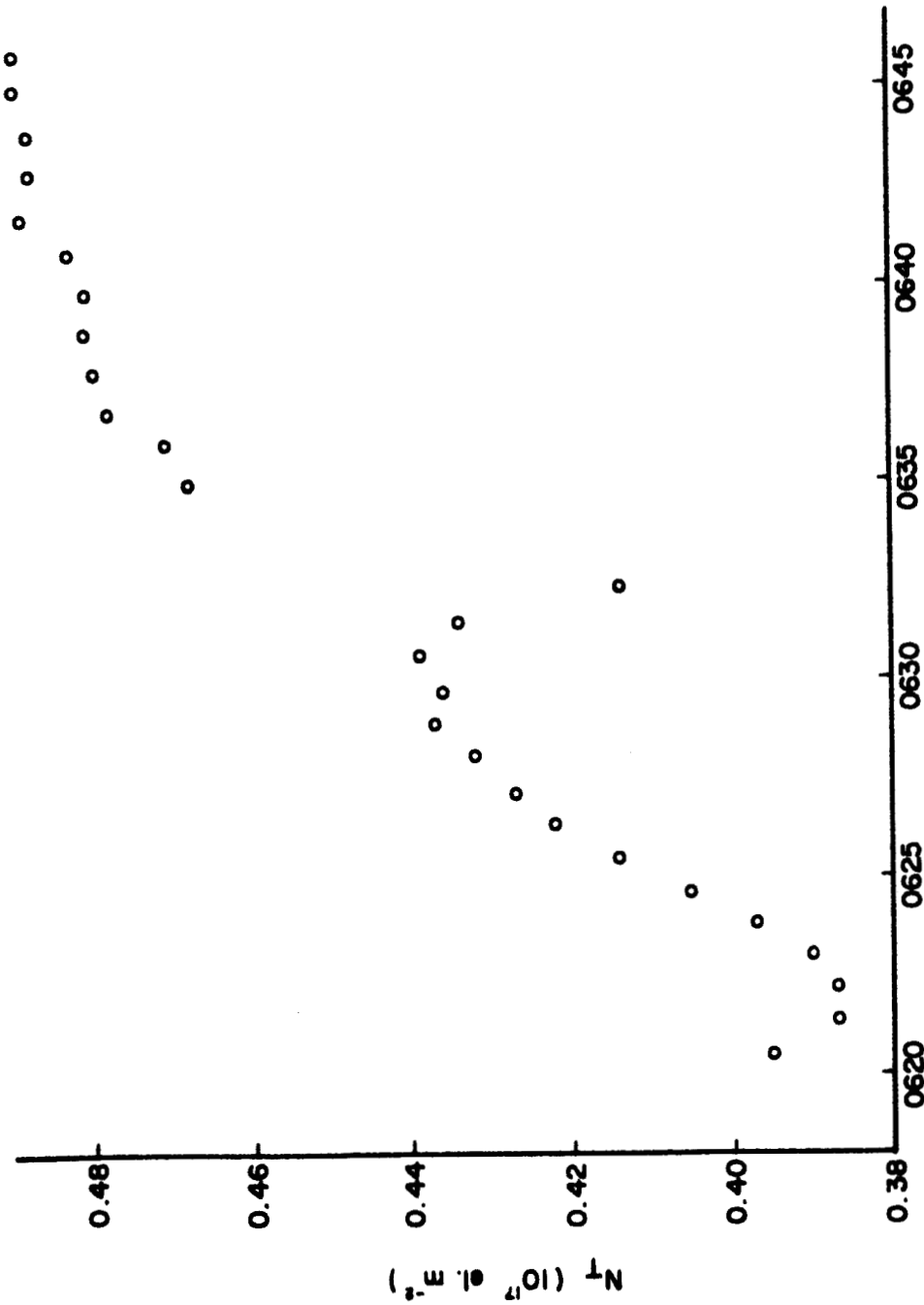

RESULT OF QUASI-TRANSVERSE ERROR 7-27-62

FIGURE 16

of these large electron content gradients with latitude and longitude this record is unsatisfactory for determining the production rate. Records of this nature may however be useful in studying the irregularities themselves. The observed irregularity may possibly result from the fact that ground sunrise does not occur until late in the record so that production is not yet well established. That is, new ionization is not great enough to remove any existing unevenness in the horizontal electron density distribution.

The record for the following day, shown in Figure 10, is a little further from sunrise but still exhibits irregularities. As indicated, scintillation occurred near the beginning and the end of the record. For interest purposes the ionospheric point latitude is included in the figure.

The following days record, Figure 11, is entirely after ground sunrise, about ten minutes at the center. With the exception of a slight "tailing off" at the far end the curve is practically linear as expected.

The records for the three day sequence in July 1962 exhibit several features which are interesting and will be discussed using the record of the first day. Aside from the scintillation which appears in the early portion of the record in Figure 12 there is considerable "tailing off" at both ends. It was found that if the $B_L \sec \chi'$ term used in calculating the electron content was evaluated for a mean ionospheric height of 400 km instead of 300 km the curve becomes nearly linear as shown in Figure 17, suggesting that the effective ionospheric height is greater than 300 km. The middle of the pass

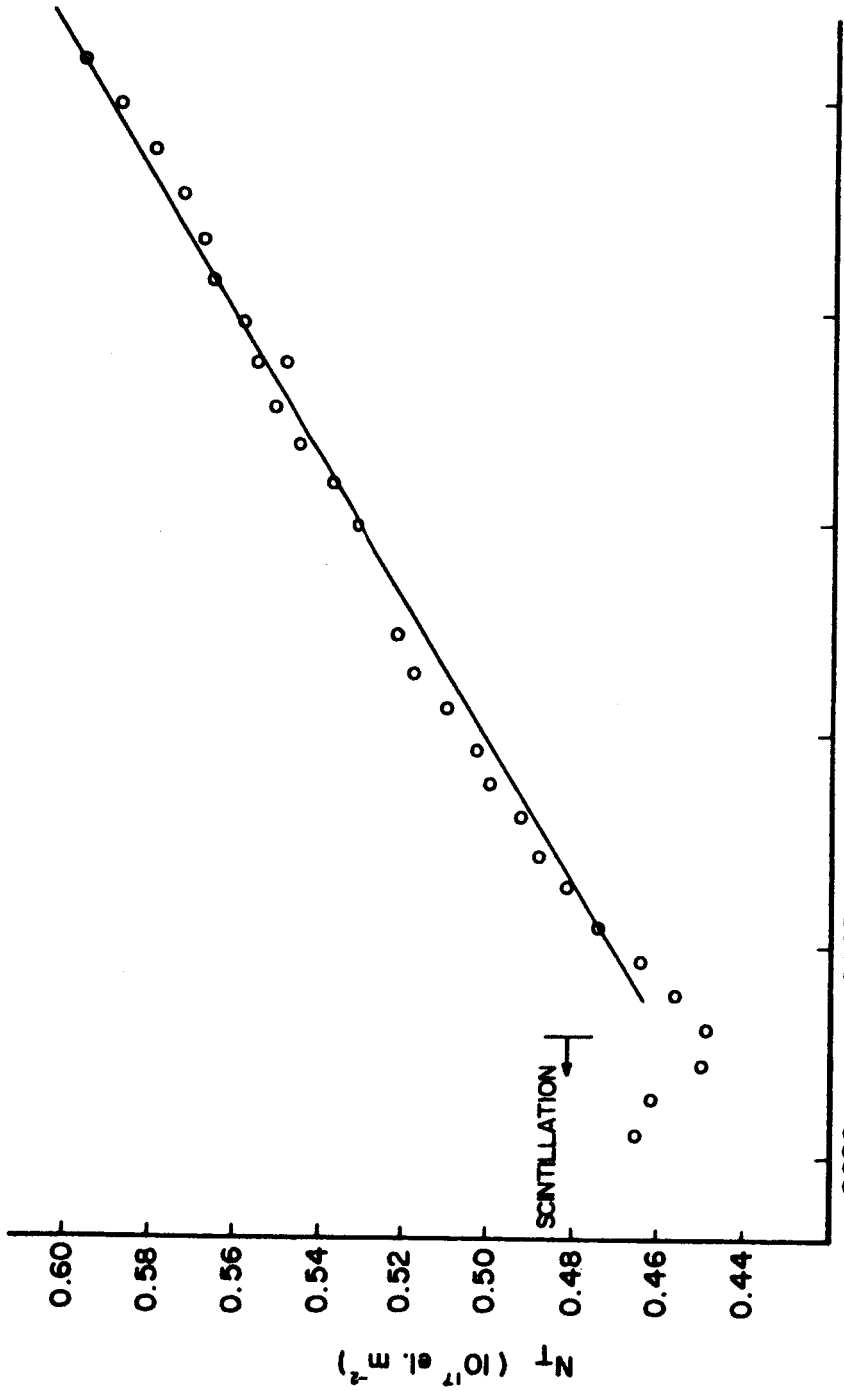

LINEAR INCREASE OF N_T WITH MEAN HEIGHT TAKEN AT 400 km 7-27-62

FIGURE 17

occurred at 0633. Inspection of the electron density profile for 0630, shown in Figure 18, however, does not confirm this idea. Apparently there is some other factor controlling this phenomenon.

In assuming that B_L sec χ' is sufficiently constant to be removed from the integral it was implied that satellite zenith angles, χ'', be relatively small, generally less than fifty degrees. Corresponding values of χ' are shown in the figures and we note that values as high as 68 degrees, corresponding to χ'' equal to 80 degrees, are reached. For χ'' equal to 50 degrees the difference in B_L sec χ' at 300 km and 350 km is approximately 8%; whereas, for χ'' equal to 80 degrees the corresponding difference is approximately 12%. This would seem to indicate the source of the "tailing off" and would imply that extreme points should be used with caution in this and other works. While this comment still applies, we do see inconsistencies such as the "tailing off" in Figure 13 where χ' is less than 46 degrees ($\chi'' < 50$ degrees) and in Figure 14 where a nearly linear curve results in spite of the variation of χ' from 29 to 68 degrees. Consequently, the precise nature of this phenomenon is not fully understood; however, useful production rates can still be obtained if these factors are kept in mind. The computed rate of change of total electron content, N_T, for each record is tabulated in Table III with the most likely rate given by (1) and an alternate rate based upon a different portion of the curve by (2). The uncertainty is generally less than 15%. The production rates, corrected by use of loss rates (g), Table II, are also tabulated.

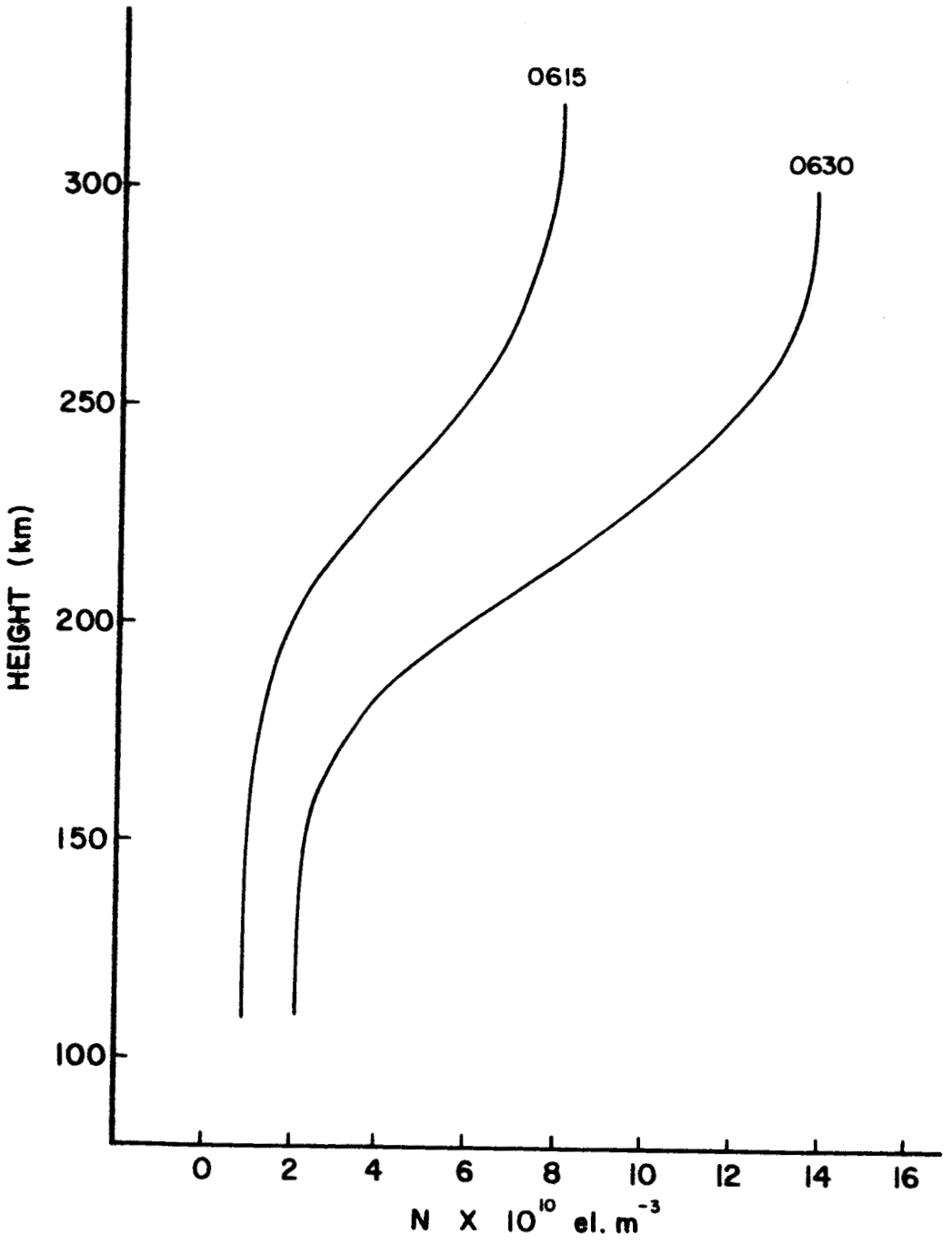

ELECTRON DENSITY PROFILE 7-27-62

FIGURE 18

Table III

Measured Increase of Electron Content and Production Rate

Ident.	9/18/61	9/19/61	7/27/62	9/28/62	7/29/62	2/25/63
		dN_T/dt 10^{13} m^{-2} sec^{-1}				
1	1.4	3.8	0.73	1.5	1.5	1.6
2		3.4	0.75	1.5		1.9
		$q_T = dN_T/dt + L_T$ 10^{13} m^{-2} sec^{-1}				
1g	1.9	4.8	1.1	2.2	2.1	3.1

Chapter VII

Experimental Results

7.1 Calculated Solar Ionizing Flux

The results of the last chapter indicate that neglecting to account for atomic oxygen loss would result in an error in excess of 20% in determining flux. Even with the uncertainties in the loss coefficients, by correcting for loss the error in the production rate undoubtedly is reduced to less than this. This figure can certainly be improved when better loss coefficients are available.

The "effective" solar ionizing flux for each record is given in Table IV below, where it was assumed that $\gamma = 1$, that is that each photon produced an electron-ion pair, and measured changes in electron content were corrected for atomic oxygen loss. This also implies that all molecular nitrogen ions are lost by the charge transfer process, so that N_2^+ electrons are included in the measured change in electron content.

Table IV

Effective Solar Ionizing Flux Incident
Upon the Atmosphere

Date	9/18/61	9/19/61	7/27/62	7/28/62	7/29/62	2/25/63
I_∞ (10^{14} photons m^{-2} sec^{-1})	2.5	5.4	1.2	2.4	2.0	1.9

The results indicate only small variations in solar flux and with the exception of one day it was approximately 2 x 10^{14} photons

m^{-2} sec^{-1}. It furthermore is estimated that the error in the flux calculations is less than 40%.

7.2 Comparison and Discussion of Results

It is interesting to note Hinteregger and Watanabe (August 1962) reported measuring a total flux of 5.9×10^{14} photons m^{-2} sec^{-1} for the 1027 to 10 angstrom range on August 23, 1961. Effective ionizing fluxes of 2.5 and 5.4×10^{14} photons m^{-2} sec^{-1} were obtained here for September 18 and 19 respectively, just a month later. For the one date the effective ionizing flux was comparable in magnitude to the total flux, in the other case it was about one half as large. The reliability of the flux for September 18 is questionable due to scintillation present in the record. Hinteregger, Hall and Schmidtke (1964) give a total flux of 6.69×10^{14} photons m^{-2} sec^{-1} for the 1027 to 10A range, of which 1.34×10^{14} ph m^{-2} sec^{-1} is in the 1027 to 911A range, as being representative of July 1963. This is about three times the effective ionizing flux found for February 1963.

Garriott and Smith (1965) made sunrise flux measurements based on Syncom III observations in Hawaii and Stanford during the autumn of 1964 and found the integrated production rate for an overhead sun to be $1.2\ (\pm 0.2) \times 10^{14}$ el m^{-2} sec^{-1} with little day to day variation. Loss contributions were neglected in this figure. However, when due allowance for atomic oxygen loss is made and an ionizing efficiency of one photon per electron is assumed, the ionizing fluxes are seen to be approximately the same as those obtained in this study. A scale height of 40 km as was used by them is insufficient to alter this condition, for we note that the flux would only

be decreased by a maximum of 10% if the scale height is taken to be 40 km instead of 30 km.

Garriott and Smith also suggested that when rapid recombination of N_2^+ is assumed the total integrated production rate, and hence the effective flux, is increased by about 60%. In Chapter V the increase was found to be 46 to 56 per cent.

Should one assume that O_2^+ electrons are included in the measured dN_T/dt, that N_2^+ recombines rapidly and use an "equivalent" ionizing efficiency factor of 0.43 (Chapter V) the calculated total fluxes will be about 2.3 times larger than the effective ionizing fluxes given in Table IV. The total fluxes computed on this basis are given in Table V.

Table V

Total flux I'_∞ for 10-1027A range, assuming N_2^+ recombines rapidly, O_2^+ electrons are measured and actual ionizing efficiency is 66%.

Date	9/18/61	9/19/61	7/27/62	7/28/62	7/29/62	2/25/63
$I'_\infty (10^{14}\,ph\,m^{-2}\,sec^{-1})$	5.8	13	2.8	5.6	4.7	4.4

If it is assumed that N_2^+ and O_2^+ recombine rapidly the "equivalent" ionizing efficiency factor would be approximately 0.34. Total fluxes calculated on this assumption are tabulated in Table VI.

Table VI

Total flux I''_∞ for 10-1027A range, assuming N_2^+ and O_2^+ recombine rapidly and actual ionizing efficiency is 66%.

Date	9/18/61	9/19/61	7/27/62	7/28/62	7/29/62	2/25/63
I''_∞ (10^{14} ph $m^{-2} sec^{-1}$)	7.4	16	3.5	7.0	5.9	5.6

While the results given in Table V and VI represent extreme cases, since the rapidity of the recombination of these molecular ions varies with altitude, they do suggest that if the photometric measurements of Hinteregger et al. are reasonably correct, three photons are required on the average to produce two free electrons. They also indicate that in general N_2^+ and perhaps O_2^+ recombine rapidly so that ionization of molecular nitrogen and possibly molecular oxygen do not contribute significantly to the increase in electron content.

For purposes of comparing the measured fluxes with other ionospheric data a plot of hourly maximum electron densities obtained from f_0F_2 data is shown in Figure 19 for the various dates considered. Although Washington, D. C. data was used, because Huancayo data was unavailable, the solar behavior indicated should be the same.

Comparison of the relative slopes around 6 A. M. with the corresponding fluxes indicates that the correlation between flux and slope is good. The steeper slopes are associated with the higher fluxes as expected. In particular, the steepest slope was on

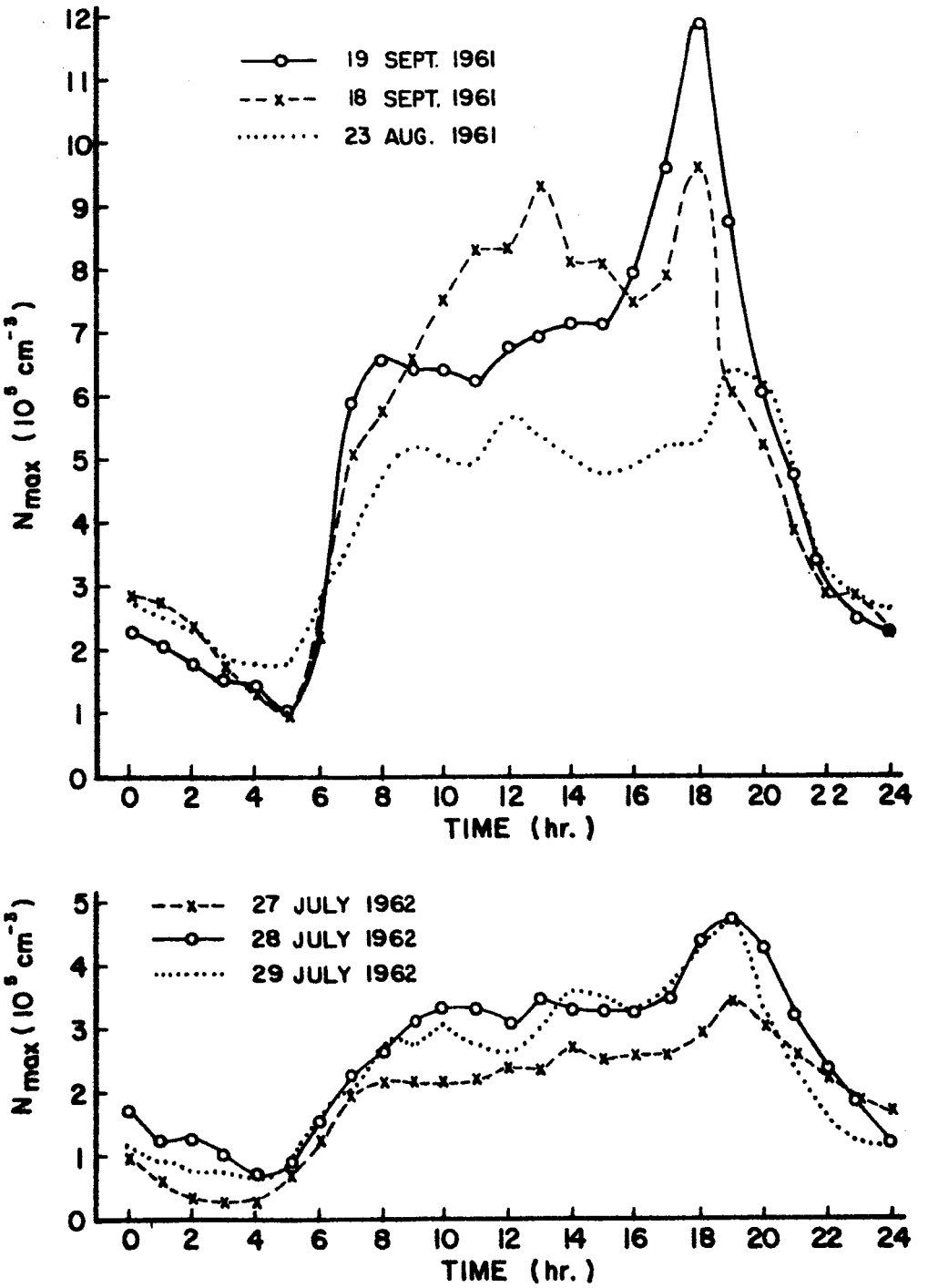

MAXIMUM ELECTRON DENSITIES
WASHINGTON, D.C.

FIGURE 19

September 19, 1961 when the flux was observed to be largest. Hence, there is some indication that the flux, which is apparently about twice as large as the modal flux, is associated with increased solar activity in the ionizing radiation spectrum.

Chapter VIII

Summary

8.1 Problem and Procedure of Investigation

A technique was developed for studying the relationship between the ionosphere and solar ionizing radiation. The method consists of measuring the change in integrated electron density by the Faraday rotation of radio signal from satellites. The solar ionizing flux is determined from the electron production rates which are arrived at by accounting for electron losses and the measured increase in electron content during sunrise at an equatorial station.

The relationship between the integrated production rate and ionizing flux was presented and discussed. Because of the complexity which results due to the chromatic radiation and multiconstituent atmosphere it is proposed that the simple theory of a single constituent atmosphere and monochromatic radiation be applied, in which the flux is an effective ionizing radiation producing an electron distribution similar to what is actually observed. This requires that an effective scale height be attributed to the atmosphere.

A model study of production due to chromatic radiation in an atmosphere of atomic oxygen, molecular oxygen, and molecular nitrogen was made for general interest and to determine the effective scale height. Based upon two semi-independent methods of determination it was concluded that for an 800°K thermosphere (S = 100), or quiet solar conditions, the effective scale height is approximately 30 km.

Various electron loss processes were considered and

conditions were selected for minimizing this contribution. Nevertheless, it was found that neglecting to account for loss due to atomic oxygen ions for the times considered would result in an error in excess of 20% in the production rate and hence in the ionizing flux. It further was shown that this loss could be calculated without extrapolation of bottomside electron density profiles.

If molecular nitrogen ions are lost by rapid recombination, rather than by charge transfer, it was noted that the measured production rate, and hence calculated flux, is increased by 46 to 56 percent. In actuality the ions are lost by both processes, however, the extent to which each occurs is uncertain.

The model study also indicated that electron production due to molecular oxygen is only about one-seventh of the total production.

8.2 Results and Conclusions

The technique was applied to data from the Transit 4-A satellite made at Huancayo, Peru during the period of September 1961 to February 1963. Analysis of the records revealed some unexplained characteristics; however, a satisfactory measure of the increase in electron content during approximately a fifteen minute time interval were obtained.

When account of the electron loss due to atomic oxygen ions, the principal ions in the F region, was made and N_2^+ was assumed to be lost by rapid charge exchange, the resulting calculated fluxes based upon an ionizing efficiency of one electron per photon, were, with one exception, approximately 2×10^{14} photons m^{-2} sec^{-1}. These

results are comparable to those obtained by Garriott and Smith (1965), if corrected for atomic oxygen loss, from similar measurements made at Hawaii and Stanford using the Syncom III transmissions. Total fluxes obtained by photometric measurements in the 10-1027 Å range are, however, two to three times larger.

It was concluded from the model study that if quasi-photoequilibrium of molecular nitrogen ions is assumed, particularly that these ions recombine rapidly, along with the result that on the average three photons are required to produce two electrons, the total fluxes would be about 2.3 times the effective ionizing fluxes, thus making the total fluxes obtained in the present work approximately the same magnitude as those obtained by photometric methods.

Indication is that if the total fluxes obtained by the photometric methods are reasonably correct, N_2^+ and possibly O_2^+ are in general lost by rapid recombination during the sunrise period.

8.3 Suggestions for Improvement and Further Research

The analysis of sunrise records revealed the unexpected non-linear increase of electron content with time, whether real or otherwise, in some records. Some possible causes were considered, but further research on this phenomenon is required.

In this work the effect of horizontal movements of ionization were neglected; however, these should be investigated and it is possible that this might in part be associated with the former observation.

For purposes of increasing data points it would be desirable

to use a lower frequency than the 54 Mc/s of Transit 4-A. Furthermore, a satellite with a lower inclination orbit would be useful in studies of this type, particularly in studying east-west gradients.

A synchronous satellite, such as used by Garriott and Smith (1965), would also be advantageous for it would not suffer from orbital precession and thus could measure electron content continuously, so as to obtain daily flux records. It further would eliminate the problem connected with horizontal gradients in electron content since the same area of the ionosphere is viewed continuously. It may suffer from a low Faraday rotation rate, which thus would limit the resolution obtainable in electron content variations with time; however, the advantages far outweigh this minor limitation.

Acknowledgements

The guidance and encouragement of Dr. William J. Ross in this study is most sincerely appreciated. The assistance of the Computress Staff of the Ionosphere Research Laboratory in performing the numerous calculations is acknowledged. Indebtedness is expressed to Mr. Peter Banks for providing the computer program for production rates.

The f_0F_2 values and electron density profiles were supplied by the Central Radio Propagation Laboratory, National Bureau of Standards, Boulder, Colorado. This work truly could not have been done without the Transit 4-A Faraday Rotation records obtained through the assistance of the Instituto Geofisico del Peru.

Support for this work came from the National Aeronautics and Space Administration under Grant NsG-114-61.

Bibliography

Browne, I. C., J. V. Evans, J. K. Hargreaves and W. A. S. Murray, Radio Echoes from the Moon, Proc. Phys. Soc. (London), Ser. B, 69, No. 441B, 901 (1956).

Chapman, S., The Absorption and Dissociative or Ionizing Effect of Monochromatic Radiation in the Atmosphere on a Rotating Earth, Proc. Phys. Soc., 43, 26 (1931a).

Chapman, S., The Absorption and Dissociative or Ionizing Effect of Monochromatic Radiation in the Atmosphere on a Rotating Earth. Part II - Grazing Incidence, Proc. Phys. Soc., 43, 483 (1931b).

Friedman, H., "Ionospheric Constitution and Solar Control" in Research in Geophysics Vol. I edited by H. Odishaw, The M.I.T. Press, Cambridge, Mass. (1964).

Garriott, O. K. and F. L. Smith, III, The Rate of Production of Electrons in the Ionosphere, Private Communication.

Harris, I. and W. Priester, Theoretical Models for the Solar-Cycle Variation of the Upper Atmosphere, NASA Technical Note D-1444 (1962).

Hinteregger, H. E., L. A. Hall and G. Schmidtke, Solar XUV Radiation and Neutral Particle Distribution in July 1963 Thermosphere, Preprint for Fifth International Space Science Symposium (May 12-16, 1964, in Florence, Italy).

Hinteregger, H. E. and K. Watanabe, Photoionization Rates in the E and F Regions, 2, J. Geophys. Res., 67, 3373 (1962).

Kasner, W. H. and M. A. Biondi, DASA Reaction Rate Meeting, Pittsburgh, June 17, 1964.

Nicolet, M., Atmospheric Model, 800 °K Thermosphere, Private Communication.

Nicolet, M. and W. Swider, The Ionospheric Conditions, Planet. and Space Sci., 11, 1459 (1963).

Quinn, T. P. and J. S. Nisbet, Recombination and Transport in the Nighttime F Region of the Ionosphere, J. Geophys. Res., 70, 113 (1965).

Ratcliffe, J. A., The Formation of the Ionosphere Layers F_1 and F_2, J. Atmos. Terrest. Phys., 8, 260 (1956).

Ratcliffe, J. A., E. R. Schmerling, C. S. G. K. Setty and J. O. Thomas, The Rates of Production and Loss of Electrons in the F Region of the Ionosphere, Phil. Trans. R. Soc., A248, 62 (1956).

Rishbeth, H., Diffusion of Ionization in the Sunrise F-layer, J. Atmos. Terrest. Phys., 20, 277 (1961).

Rishbeth, H. and C. S. G. K. Setty, The F-layer at Sunrise, J. Atmos. Terrest. Phys., 20, 263 (1961).

Swider, W., Sunrise Geometry and Optical Depth Factor, Sci. Report 164, Ionosphere Research Laboratory, Pennsylvania State University (1962).

Swider, W., The Ionic Structure of the Ionosphere, Sci. Report No. 201, Ionosphere Research Laboratory, Pennsylvania State University (1963).

Tousey, R., The Extreme Ultraviolet Spectrum of the Sun, Space Sci. Rev., 2, No. 1 (1963).

Watanabe, K. and H. E. Hinteregger, Photoionization Rates in the E and F Regions, J. Geophys. Res., 67, 999 (1962).

Wilkes, M. V., A Table of Chapman's Grazing Incidence Integral Ch(x, χ), Proc. Phys. Soc., 67, 304 (1954).